LARGE-SCALE TEST ON SODIUM LEAK AND FIRE (Ⅲ)

(Large-Scale Sodium Spray Fire Test in Air, Run-E1)

June, 1987

OARAI ENGINEERING CENTER

POWER REACTOR AND NUCLEAR FUEL DEVELOPMENT CORPORATION

動力炉・核燃料開発事業団（Power Reactor and Nuclear Fuel Development Corporation）

PNC-TN9410 86-124 Tr
1987年 6 月

大規模ナトリウム漏洩燃焼試験（III）

— 空気雰囲気における大型ナトリウム・スプレー燃焼試験, Run-E1 —

森井 正*・福地 平*・山田敏雄*・姫野嘉昭*

要 旨

〔目的〕FBRの設計基準のナトリウム漏洩事故で想定されている空気雰囲気におけるナトリウム・スプレー燃焼について，従来と比べてより長時間かつ大型施設での試験を行い，コード検証用の実験データベースの拡充を計る。

〔方法〕サファイア施設の鋼製密閉試験容器SOLFA－2（内容積：111 m^3，ステンレス製）を用い，ナトリウム量1,000 kg，スプレー流量510 kg/sec，スプレー継続時間30分，流出ナトリウム温度505℃，スプレーノズル高さ4 mで試験を行った。

〔結果〕試験開始と共に雰囲気ガスの温度および圧力は急上昇し，1.2分後にはそれぞれ700℃と1.24 kg/m^2Gとなった。内部の酸素は，約4分後には完全に消費された。酸素消費速度から求めた燃焼速度は160 g-Na/secで，これはスプレー・ノズルからの流出ナトリウム流量の約30%に相当する。容器内部に設置した多数の熱電対は，スプレー燃焼時の約1,000℃近くの高温のため損傷した。燃焼時の激しい自然対流のため，容器内高さ方向の酸素濃度分布は均一であった。ナトリウム・エアロゾル濃度は，最高17.5 g-Na/m^3が5分後に検出されたが，その後は減少し，20分後には1 g-Na/m^3まで低下した。

〔結論〕長時間，大型施設による試験で，燃焼速度，エアロゾル濃度などについて従来とほぼ同様な結果を得た，コード検証用の実験データベースが拡充された。

＊ 安全工学部プラント安全工学室

PNC-TN9410 86-124 Tr
June, 1987

Large-Scale Test on Sodium leak and Fire (III)
(Large-Scale Test of Sodium Spray Fire in Air, Run-E1)

Tadashi Morii*, Taira Fukuchi*,
Toshio Yamada*, and Yoshiaki Himeno*
Text edited by T. Morii

Abstract

A large-scale sodium spray fire test (RUN-E1) has been conducted in an air atmosphere using the SOLFA-2 test vessel (111 m^3 made from SUS304) of the SAPFIRE facility.
The major test conditions are as follows:

Spray Rate	510 g/sec
Spray Period	1800 sec
Sodium Temperature	505 °C
Spray Falling Height	4 m

As sodium spray started, the gas pressure and temperature rose rapidly and reached maximums of 1.24 kg/cm^2 -g and 700 °C after about 1.2 minutes. The oxygen in the test vessel was consumed completely after 4 minutes. From the oxygen consumption rate, the burning rate of sodium was calculated to be 160 g-Na/sec, equivalent to about 30% of the sodium spray rate (under the assumption of 100% Na_2O_2 production).

Many thermocouples installed in the spray core region failed due to

---

* Plant Safety Engineering Sec., Safety Engineering Div., OEC

the high temperature (above 1000 °C), which suggested the existence of a burning zone around the sodium droplets.

No remarkable vertical concentration distribution of oxygen was observed in the vessel during the spray, indicating that the gas in the vessel was well mixed by natural convection due to gas temperature difference between the outside and the inside of the spray core.

Aerosol concentration reached a maximum of 17.5 g/Na/m^3 after 5 min then decreased below 1 g-Na/m^3 after 20 min.

TABLE OF CONTENTS

List of Tables

List of Figures

1. INTRODUCTION

In the prototype reactor Monju, a sodium spray fire from a leak hole having a diameter equivalent to 1/4 Dt of the sodium piping is postulated as the design basis sodium leak accident. The temperature and pressure transients in the event of such an accident were analyzed using the sodium fire analysis code, ASSCOPS.

ASSCOPS has been validated[1] by spray fire experiments[2),3]. However, the spray durations were short (less than 20 seconds) in these experiments. Therefore, a longer and larger-scale spray fire test was recommended for realistic evaluation of the accident. Table 1.1 compares the scale of the sodium spray fire tests conducted so far together with the present test and the design basis sodium leak accident in Monju.

This report presents a long-duration and large-scale spray fire test which is called Run-E1. In the second chapter of the present report, the SOLFA-2 test vessel is explained. A water spray test, which aimed to determine the droplet size distribution of the generated spray, is also presented in it. The third chapter describes the test procedure and test conditions of Run-E1. The fourth contains the test results and discussion, and the fifth presents the conclusion.

2. TEST APPARATUS

2.1 Test Rig

The large-scale sodium leak and fire test facility used in the present test consists of a sodium heater, a test vessel named SOLFA-2, a storage tank, a drain tank, and a nitrogen gas supply system. This test rig is a part of the SAPFIRE facility. Figure 2.1 shows the flow diagram. The components are explained below.

2.1.1 Sodium Heater

The sodium heater heats sodium up to the test temperature and pressurizes sodium. Sodium is supplied to SOLFA-2. The sodium supply flow rate is controlled by controlling its cover gas pressure and is measured by an electromagnetic flow meter installed in the middle of the sodium piping that connects the sodium heater with the test vessel.

The specifications of the sodium heater are given below.

Sodium heater specifications

Type	A vertical cylindrical container with an upper flange.
Inner volume	5.36 m^3
Dimensions	1300 mm(ID) × 4300 mm(H)
Thickness of outer wall	10 mm
Material	SUS 304
Heater capacity	70 kW (200 V-AC, 3 ϕ, 50 Hz)
Max. working temperature	550 °C
Max. working pressure	5 kg/cm^3 g

2.1.2 Storage Tank

The storage tank stores the sodium used for the test. If needed, the sodium in the storage tank can be purified by operating a cold trap. Its specifications are given below.

Sodium tank specifications

Type	Vertical cylindrical container
Capacity	20 m^3
Dimensions	2500 mm(ID) × 4480 mm(H)
Thickness	14 mm
Material	SUS 304
Max. working temperature	550 °C
Max. working pressure	5 kg/cm^2 g

2.1.3 Drain Tank

After the experiment, the sodium collected below the fire suppression plate is returned to the drain tank through the drain piping at the bottom of the test vessel.

The drain tank is a horizontal cylindrical container installed in the floor pit of the test building. Its specifications are given below.

Drain tank specifications

Type	Horizontal cylindrical container
Capacity	6 m^3
Dimensions	1500 mm(ID) × 3582 mm(H)
Thickness	9 mm
Material	SUS 304
Max. working temperature	450 °C
Max. working pressure	3 kg/cm^2 g

2.1.4 Nitrogen Gas Supply System

The nitrogen gas supply system controls the cover gas pressure in the sodium heater, the test cell, the storage tank, and the drain tank. This system also serves as a vacuum system. During tests, the system controls the gas pressure in the heater to supply a constant sodium flow rate to the test vessel through a spray nozzle. It also supplies the inert gas to the test vessel after the test.

The nitrogen gas supply system specifications are given below.

Nitrogen gas supply system specifications

Material	SGP
Piping	2 inches
Max. working pressure	5 kg/cm^2 g
Fluid	Nitrogen gas

2.2 Outline of Test Vessel SOLFA-2

The specifications of SOLFA-2 and its components including the fire suppression plate and the sodium spray nozzle will be explained below. Figure 2 shows the construction of the SOLFA-2 test cell.

2.2.1 SOLFA-2 Vessel

SOLFA-2 is a stainless steel, vertical cylindrical vessel with a volume of 111 m^3. It has a maintenance manhole fixed to its body and the upper flange with bolts and nuts. The sodium spray nozzle, the fire suppression plate and the fire suppression bucket are installed in it. The body is covered with a water cooling jacket to protect the vessel from the over-heating and over-pressure due to a spray burning. A rupture disk is provided to release over-pressure, if necessary.

The specifications of the test cell, the water cooling jackets, and the rupture disk are shown below.

Test cell specifications

Type	Vertical cylinder with a flange for opening the top.
Capacity	
Total volume	111 m^3
Volume above the fire suppression plate	95.5 m^3
Volume below the fire suppression bucket	15.5 m^3
Dimensions	3600 mm(D) × 10816(H)

Wall thickness	25 mm
Material	SUS 304
Max. working temperature	400 °C
Max. working pressure	2 kg/cm^2 g

Water cooling jacket specifications

Type	Double cylindrical container
Volume	6.18 m^3
Dimensions	3800 mm(OD) × 3659 mm(ID) × 7040 mm(H)
Thickness	6 mm
Material	SS 41

Rupture disk specifications

Type	A reversible type (mfd. by Niigata BS & B Safety System Inc. RB-90)
Material	Nickel/alloy 200
Size	8 inch
Design rupture pressure	1.71 kg/cm^2

2.2.2 Fire Suppression System

The purpose of Run-E1 is to obtain the data on a spray burning. A fire suppression system is provided at the bottom of the vessel to minimize the influence of pool burning.

As shown in Fig. 2.3, the fire suppression system consists of a fire suppression bucket made of carbon steel (SM4128) and a fire suppression plate made of common carbon steel (SS41). The spray sodium from the nozzle burns and drops onto the fire suppression plate.

The sodium which dropped onto the fire suppression plate flows into the fire suppression bucket along the 1/100 slope and is self-extinguished there.

The mechanism of the self-extinguishment within the fire suppression bucket is explained in Fig. 2.4.

The specifications of fire suppression system are given below.

Fire suppression system specifications

(1) Fire suppression bucket

Material	SM41B
Dimensions	3400 mm(ID) × 250 mm(H)
Thickness	6 mm

(2) Fire suppression plate

Material	SS41
Diameter	3400 mm

2.2.3 Sodium Spray Nozzle (Fig. 2.5)

The sodium spray nozzle specifications are shown below.

Sodium spray nozzle specifications

Material	SUS 304
Number of nozzles	1
Spray cone angle	35 °
Height of spray nozzle	3980 mm

The diameter of the sodium droplets generated by the spray nozzle was determined in a spray performance test using water. The volume mean diameter determined was 2 mm.

Fig. 2.6 shows an outline of the spray nozzle test using water and its results.

2.3 Measuring Instruments

The data to be obtained in Run-E1 are the temperature transient at each part of the vessel, the heat fluxes, the pressure transients, the oxygen concentration changes, and the aerosol concentration resulting from the spray burning. Their measurements will be explained below.

(1) Measuring the temperature transients at each part of the vessel

As shown in Fig. 2.7, thermocouples for measuring the temperature were placed at 15 points within the spray cone, and the 10 sets of three thermocouples were placed outside of the spray cone.

The thermocouples in the spray cone measure the temperatures of the sodium liquid droplets, their flame, and the gas. These temperatures, however, are difficult to distinguish from one another and are mixed somewhat in the measurement results.

With each set of three thermocouples outside the spray cone, the correlation of one thermocouple to another is determined, then the gas convection velocity is determined from the function at their respective positions. The time constant of thermocouple is comparatively large, therefore, fast gas velocity cannot be measured. The sets of thermocouples were therefore placed at 10 positions. The distance between thermocouples in a set was varied from 5 cm to 20 cm, so as to find the optimum spacing.

Five thermocouples were placed in the fire suppression bucket to measure the depth and temperature of the sodium in it, three to measure the volume and temperature of the sodium within the bucket, and two to measure the temperature of the fire suppression bucket.

Furthermore, a total of 29 thermocouples were installed to measure the temperatures of the vessel walls and of the water-cooling jacket.

All thermocouples are grounded type C-A (chromel-alumel) thermocouples with a diameter of 1.0 mm.

(2) Measurement of the radiation heat flux

To measure the convective and the radiative heat transfer from the high-temperature spray cone to the vessel wall, two heat flux meters were attached side by side at the same position (at the same height as that of the spray nozzle) on the wall surface. One of them was covered with a shield plate to shield from the radiation (Fig. 2.8 shows these meters) and to measure only the convective heat flux. The heat flux due to radiation was determined from the difference of the measured values by the two meters.

(3) Measurement of the oxygen concentration change

The spray burning rate during a test is determined from the oxygen

concentration changes within the test vessel. The oxygen concentration was measured by two magnetic oxygen concentration meters; a gas chromatograph, and an automatic gas sampling device.

When a sodium spray burns in the lower half of SOLFA-2, oxygen concentration distributions may vary in the vertical direction. An automatic sampling device was therefore placed in the upper part of the test vessel, a magnetic oxygen concentration meter in the middle part, and an other magnetic oxygen concentration meter and an on-line gas chromatograph in the lower part to measure the oxygen concentrations in the respective areas.

Figure 2.2 shows the arrangement of these oxygen concentration measuring instruments, of which specifications are shown below.

1. Magnetic oxygen concentration meter

Type	6395 type magnetic oxygen analyzer (mfd. by Mitaka Industries, Ltd.)
Measuring range	0 to 25 vol%
Response	About 20 sec/90% response (an independent analyzer)
Indication	Continuous

2. On-line gas chromatograph

Type	370T type oxygen & hydrogen analyzer (mfd. by Gas Chromatography Inc.)
Column	Molecular sieve
Resolution	1 to 30%
Indication	An intermittent measurement system (minimum interval of 5 minutes)

3. Automatic gas sampling device

The automatic gas sampling device samples the gas into a 2,000 cc cylinder through the gas sampling nozzle provided at the vessel. The sampling interval can be freely set by a timer. There can be a maximum of 15 sampling cylinders.

The gas is analyzed by taking the sampled gas from the automatic sampling device and putting it in the gas chromatograph.

(4) Measurement of transient gas pressure in the vessel

The atmospheric gas pressure transients within the vessel associated with sodium burning were measured by a pressure gauge at the upper part of SOLFA-2. This pressure gauge was also used to generate a feedback control signal to maintain a constant differential pressure between the test vessel and the sodium heater and thus supply a constant sodium flow rate to the test vessel. The pressure gauge specifications are shown below.

Pressure gauge specifications

Type	An electronic pressure transducer (mfd. by Yokogawa Hokushin Electric Co., Ltd.)
Measuring range	-1 to 3 kg/cm^2 g
Measurement precision	+ -0.25% of full scale

(5) Observation instrument

To observe the sodium spray burning, video cameras were placed so as to view the spray nozzle from the upper part of the test vessel and from the side of the spray nozzle.

(6) Measurement of the mass and composition of the reaction products

The concentration of the aerosol generated by the spray burning, the mass of the setting aerosol, and the mass of the aerosol deposited on the wall were measured in the following ways:

1. Aerosol concentration was measured by taking the gas sample from time to time by an automatic aerosol sampler. About 2,000 cc of gas was sucked by the sampler and filtered through a sintered filter having a two-micron-meter pore size to collect the aerosol. The filtered aerosol was then dissolved in water, and its sodium content was determined by titration with the standard acid solution.
2. The settling aerosol flux was measured by the settling aerosol sampler. The settling aerosol on the plate was collected. The mass of aerosol collected was determined by atomic absorption analysis or by titration after dissolving the collected aerosol in water.
3. After the test, 50 cm^2 area of the aerosol deposits on the inner wall of the test vessel were scraped off from various parts of the wall and

subjected to quantitative analysis.

The combustion products from sodium remaining in the fire suppression bucket were weighted and the remaining sodium thickness was measured.

The signals of temperature, the radiation heat flux, the oxygen concentration by the magnetic oxygen meter, the gas pressure within the vessel, and the sodium spray flow rate were recorded using a computer (HP1000).

3. TEST METHOD AND CONDITIONS

3.1 Test Method

Table 3.1 shows the test procedures of Run-E1, which was conducted on September 1985.

First, the sodium in the sodium heater was heated to the predetermined temperature. Next, the pressure difference between the cover gas of the sodium heater and that of the test vessel was controlled. After these, the sodium valve at up-stream from the spray nozzle was opened, then sodium was supplied to the spray nozzle.

The test data was recorded on a magnetic tape using a degital data acquisition system for 11 hours from the start of sodium spray. The data recording interval was 50 msec (20 Hz) during the first one hour and 500 msec (2 Hz) for the last 10 hours. Two video cameras were operated to observe the spray form and spray burning.

The sodium spray was terminated when the total sodium mass reached 920 kg (determined by integrating the sodium flow rates over time).

After the termination of the sodium supply, the automatic aerosol sampler and the automatic settling aerosol sampler were started taking care not to disturb the gas convective flow within the test vessel.

The sodium recovered within the fire suppression bucket was drained into a the impurities sedimentation tank after it cooled below 450 °C.

After the temperatures of the sodium combustion products in the test vessel cooled to the room temperature, about 50 kg of dry ice (CO_2) was thrown into the vessel to stabilize the sodium. The manhole was then opened to collect the remaining sodium and aerosol to measure their weight.

3.2 Test Conditions

The test conditions are summarized in Table 3.2. The rationale for these conditions is shown below.

(1) Sodium temperature : 505 °C

This temperature corresponds to the rated operating conditions of the Monju secondary cooling system.

(2) Sodium spray flow rate : 36.7 /min

This was determined based on the results of pre-analysis using a mean droplet size from the water spray test. This flow rate may generate the maximum permissible pressure in SOLFA-2 due to the combustion.

(3) Total sodium supply mass : 1 ton

This was determined to facilitate sodium disposal.

(4) Spray expansion angle : 40-degree

Though the spray expansion angle depends on the characteristics of the spray nozzle, this is the maximum angle at which no generated spray droplet strike the inner wall of SOLFA-2.

4. RESULTS AND DISCUSSIONS

4.1 Gas Pressure

Fig. 4.1 shows the gas pressure transient together with the sodium spray flow rate.

The gas pressure rapidly increased with the start of spray burning, reaching a maximum of 1.24 kg/cm^2 -g about 1.2 minutes after, then decreased slowly. At 350 seconds, a slight change was observed in the pressure decreasing rate. This is because the sodium flow rate suddenly increased. As mentioned previously, the spray flow rate was intented to keep constant by controlling the cover gas pressure of the sodium heater and by adjusting of the sodium valve opening ratio automatically. However, this was unsuccessful, so the actual control was made manually resulting slight changes in the flow rate.

4.2 Gas Temperature

Many thermocouples were placed in the test vessel, as shown in Fig. 2.7. Figure 4.2 shows the results of measurement made by the thermocouples in the gas space. The gas temperature (B) (thermocouple TE-2082) inside the spray cone rapidly rose beyond 1,000 °C after the start of sodium spray. Meanwhile, the gas temperature (A) (TE-2085) outside the spray cone reached a peak of over 700 °C at the upper part of the vessel and exceeded 600 °C even on the vessel side (C). The high gas temperature in the upper part (A) would be caused by the heated gas which rose by buoyancy.

A more detailed examination will be made on temperatures (A), (B), and (C). There are many thermocouples in the gas space above the spray nozzle. Figure 4.3 shows the outputs of those thermocouples (TE2040, 2041, 2042, 2046, 2052 and 2058) on the center line, and Fig. 4.4 shows the outputs of those (TE2043, 2044, 2049, 2055 and 2061) on a line laterally 90 cm away from the center line. As can be seen from these figures, gas temperatures from these thermocouples were nearly equalling on upon another, and gas temperature on the center line showed almost the same behavior as on the other line. This suggests that the gas was well mixed by a strong convec-

tion in the space above the spray nozzle, and there was nearly uniform temperature distribution.

Below the spray nozzle, the thermocouples are arranged as shown in Fig. 4.5 to estimate the scope of extension of the sodium spray droplets during their falling. Sodium spray drops can naturally be expected to collide with the thermocouples below the spray nozzle. Consequently, the thermocouples marked with (F) (i.e., TE-2075, 2076, 2077, 2078 and 2080) in Fig. 4.5 were burnt and damaged during the spray experiment.

Figure 4.6 shows the outputs of the four thermocouples (TE-2082, 2083, 2084, and 2085) arranged at the fourth level from the top, i.e. 3.114 m down from the nozzle, and Fig. 4.7 shows those of the five (TE-2027, 2086, 2087, 2088, and 2089) thermocouples arranged at the 5th level, i.e. 3.984 m down from the nozzle. The figures indicate that the maximum temperature exceeded 1,000 °C. Because the boiling point of sodium is about 900 °C, these temperatures should be those of flames in the burning zone around the sodium droplets. Furthermore, the temperature in the spray cone rapidly dropped 200 to 300 seconds after the start of sodium spray because oxygen had completely been consumed around that time, as mentioned later.

The spread of the falling sodium spray droplets can be estimated using these temperature distributions.

It is reasonable to think that a spray droplet touched the thermocouple if the temperature shown is over 800 to 900 °C, considering that the maximum gas temperature in the space above the nozzle is about 800 °C and that the boiling point of sodium is about 880 °C. Based on this and Fig. 4.6, the border of the spread spray droplets can be judged to lie between TE-2083 and 2084 in Fig. 4.5 or near TE-2087 in Fig. 4.7. Figure 4.8 shows the temperatures of the remaining three thermocouples which survived. The figure indicates that the sodium spray passed over TE-2079 and 2081.

From this, the zone occupied by the spray droplets is estimated as shown by the dotted line in Fig. 4.5. The falling zone is formed in a church bell shape rather than a conical shape. Figure 4.9 shows the gas temperature distribution in the test vessel 40 seconds after the start of sodium spray. This figure clearly shows the sodium spray (the nozzle position is represented by and the sodium is falling upward in the figure). In the figure, the temperature differs even within the spray zone and is lower at the center than at the edge. This is probably attributed to the

oxygen concentration depletion by the burning in the inner part of the spray cone, which then reudces the burning rate. This is the same phenomenon as observed in a candle flame.

4.3 Temperatures of Structural Components

Figure 4.10 shows the outer surface temperatures of the ceiling (A) and side wall of the test vessel (B). At the ceiling, the temperature rose to a maximum of 130 °C, while at the side wall, it rose only 10 °C due to the water cooling jacket.

Figure 4.11 shows the temperature of the structural material around the protection steel, which prevents the high-temperature sodium droplets from directly contacting the vessel wall. Shown in the figure are the inner surface temperatures of the protection steel and the test vessel, which are strongly affected by the gas temperature at just inside the steel surface. The figure indicates that the temperature is higher in the upper part than in the lower part. Furthermore, there is a temperature difference between the steel and the test vessel (about 200 °C) for TE-2011, and about 150 °C for TE-2026 and TE-2014.

Figure 4.12 shows the outer surface temperature of the lower plate of the fire suppression system. The temperature at the center of the bottom plate of the system is about 600 °C at the highest, exceeding the spray sodium temperature of 505 °C. The temperature at the periphery of the plate is lower than that at the center because of the heat loss to the supporting structures. Many other thermocouples were arranged in the system to measure the sodium temperature, but they were burnt as the sodium liquid front (i.e., the hot burning face) passed over their lead wires.

Figure 4.13 compares the surface temperatures inside and outside the ceiling of the test vessel; the temperature difference T between the inside and outside surfaces initially exceeded 300 °C. As the vessel is 25 mm thick at the ceiling, the het flux across the wall of ceiling at that time becomes:

$$q \simeq \frac{14}{25\times10^{-3}} \times 300 = 17\times10^{3} \quad \text{kcal/m}^2\cdot\text{hr}$$

This is 10 times as large as the maximum heat flux (14,000 kcal/m^2•hr) measured in the test (see the next section). This difference may be attributed to the fact that the top of the thermocouples in the vessel are only point-welded to the wall, so they are more likely to have measured the gas temperature near the wall. This value is therefore shown here only as reference data.

In the future, such procedures as providing a groove in the wall and burying the top of each thermocouple into the groove in order to measure the inner wall surface temperature with accuracy should be taken.

4.4 Heat Flux to the Wall

As mentioned in Chapter 2, two heat flux meters were placed side by side on the inner wall of the test vessel to measure the radiative and convective heat flux during the spray. Figure 4.14 shows the resuts obtained.

The natural convection heat transfer in a vertical plate is given by the expressions below.

$$Nu_m = 0.56\ (Gr_H \cdot Pr)\ 1/4$$

$$10^5 < Gr_H \cdot Pr < 10^{11}$$

$$Nu_m = 0.021\ (Gr_H \cdot Pr)\ 2/5$$

$$10^8 < Gr_H \cdot Pr < 10^{14}$$

In the present test, the representative length was 9 m, the gas temperature was 700 °C (maximum), and the wall temperature was 100 °C, therefore,

$$Gr \cdot Pr \simeq 1.5 \times 10^{12}$$

From the above, Nu_m becomes about 2,000. Convective heat flux is determined from this as

$$q \simeq Nu \frac{\lambda}{L} \Delta T = 2000 \times \frac{0.03}{9} \times (700-100) = 4000 \quad kcal/m^2 \cdot hr$$

where, λ is the thermal conductivity of air.

The result is only about 1/3 of the max. q_{conv} (11,000 kcal/m^2•hr) shown in Fig. 4.14. It is considered that this is because the aerosol suspended in gas at such high temperatures as 700 °C releases considerable radiation energy. Exposure of the heat flux meter to the multiple scattered thermal radiation due to aerosols could not be prevented by the shield plate. The q_{conv} therefore includes the radiation energy. (The gas can freely pass inside the shield plate.)

Let the emissivity of the aerosol suspended in the gas be ε_g. The radiation energy from the gas is then expressed as,

$$q \simeq \varepsilon_g \times 4.88 \times [(700+273)/100]^4 = 44000 \times \varepsilon_g \quad \text{kcal/m}^2\text{•hr}.$$

Assuming $\varepsilon_g = 1$, q becomes maximum (44,000 kcal/m^2•hr). Though the actual ε_g is unknown, the q_{conv} in Fig. 4.14 is assumed to contain the radiation heat flux from this gas, too.

The upper limit of ε_g can be estimated to be (14000-4000)/44000 = 0.23 because the maximum heat flux determined by the heat flux meter without the shield plate was about 14,000 kcal/m^2•hr.

4.5 Oxygen Concentration Change

As mentioned in Chapter 2, an automatic gas sampler is provided at the upper part of the test vessel and a magnetic oxygen concentration meter at the middle and another one at lower parts to measure oxygen concentration distributions in the vertical direction. The magnetic oxygen concentration meter has an advantage over the automatic gas sampler in its ability to continuously measure the oxygen concentration. It has some delay in the measurement, however, because the test vessel has to be connected with the measuring instrument by a gas line. So, the delay was compensated and the corrected as shown in Appendix A.

Figure 4.15 shows the corrected oxygen concentration changes. As can be seen from the figure, values (B) and (C) measured by the magnetic oxygen concentration meter include a time delay of about 3 minutes, but the data (A) by the automatic gas sampler method contains no time delay. The time delay of this 3 minutes is considered uncorrectable by the method mentioned

in Appendix A. Important thing in the oxygen concentration changes is their decreasing rate that is closely related to the oxygen consumption rate. As shown in the figure, the oxygen consumption rate is nearly equal at the middle and the lower parts of the vessel but is slightly higher at the upper part. It is unclear whether this difference is attributed to the difference of measuring methods or is reflecting some physical phenomenon*.

This difference, however, is not so large, so we can consider that the spatial oxygen concentration sidtribution was generally uniform as a first approximation.

From this figure, we can judge that all oxygen in the vessel is consumed in about 4 minutes.

SOLFA-2's capacity is 95.3 m^2. If the burning reaction is assumed to be a 100% sodium peroxide producing reaction, the sodium burning rate is calculated as below, by using the data which maximizes the oxygen consumption rate.

$$2Na + O_2 \longrightarrow Na_2O_2$$

$$95.5 \times \frac{273/293}{22.4\times10^{-3}} \times 0.21 \times 2/(4\times60) \times 23 = 160 \quad \text{g-Na/s}$$

This rate corresponds to about 30% of the spray sodium flow rate (519 gNa/s).

4.6 Aerosol Concentration Change

The aerosol concentation changes within the test vessel were determined from the samples taken by the automatic aerosol sampler. The results are shown in Fig. 4.16. The maximum aerosol concentration was about 20 g-Na/m^3. After 20 minutes, the concentration decreased to 1 g-Na/m^3 due to settling and deposition. Figure 4.17 shows the measurement results for the mass

---

* More accurately, the gas with a lower oxygen concentration in the spray cone is carried to the upper part by convection and makes the oxygen concentration decrease more rapidly in the upper part than in the middle and lower parts.

settling flux to the floor.

4.7 Gas Flow Velocity Distribution

The gas velocity in the test vessel (regions other than the spray cone) can be evaluated by calculating the correlation functions among thermocouples.

The gas temperature fluctuations are measured by two thermocouples spaced a certain distance from each other, and their correlation functions is determined from the two different temperature fluctuation signals. When the temperature fluctuation moves from T_1 to T_2 with a velocity V in the figure below, the relation between the temperature is expressed as

$$T_2(t) \simeq T_1(t - \frac{D}{V})$$

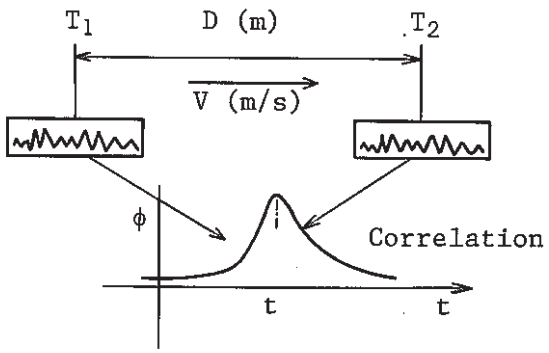

Thus the correlation function is defined as below.

$$\phi \simeq \frac{1}{T}\int_0^T T_1(t - T)T_2(t)dt$$

When the first equation above is substituted into the second equation, it becomes

$$\phi(t) \simeq \int_0^T T_1(t - T)T_1(t - \frac{D}{V})dt$$

As this is autocorrelation function of signal T_1, it will be the maximum when t = D/V.

The value D/V can be determined by calculating $\phi(t)$ and reading its maximum.

As shown in Fig. 2.7, the thermocouples are placed at 10 points in the space above the spray nozzle. Each three are circumferentially and vertically spaced to determine the gas velocities in the circumferential and vertical directions.

Figures 4.18 and 4.19 show the gas flow patterns 1, 2.5, 5, 10, 20, and 27 minutes after the start of spray that were determined in this way. As shown in the figures, the flow patterns are complicated and change with time. The driving force of the flow depends on the balance between the downward force of the sodium spray and the buoyancy force of the high-temperature gas within the spray cone. The force to pull the gas downward with the sodium spray mainly depends on the sodium flow and can be regarded as almost constant during the experiment. Consequently, the gas flow is considered to change its patterns as shown in the figures as the buoyancy due to the temperature difference between the upper and lower parts of the spray cone changes with time.

Figures 4.20 and 4.21 show the gas flow vectors determined based on the correlations among the thermocouples. Figure 4.18 and 4.19 were estimated based on this data.

5. CONCLUSION

A large-scale sodium spray fire test in an air atmosphere, Run-E1, was conducted as the first sodium fire experiment using the SOLFA-2 test vessel of the SAPFIRE facility. The spray nozzle used was what is called a full-cone type. Its characteristics were studied in the water test prior to the present sodium test. From the water test, the values of important experimental parameters were obtained as shown below. Furthermore, a pre-test calculation by the sodium fire analysis code was made using these values to evaluate the safety of the experiment in advance.

The spray flow rate	36.7 ℓ/min
Average droplet size	1.6 mm (average area diameter) 2.2 mm (average volume diameter)
Cone expansion angle	36 °

The following sodium test conditions were set up considering the pre-test analysis results:

Spray flow rate	36.7 ℓ/min
Spray time	1800 sec
Spray sodium temperature	505 °C
Spray failing height	4 m

The experiment was completed satisfactorily without trubles and following results were obtained:

(1) Immediately after the start of sodium spray, the gas pressure rapidly increased, reaching a maximum of 1.24 kg/cm^2 g after 1.2 minutes.

(2) The temperature within the spray cone exceeded 1,000 °C, and the existence of a high-temperature burning zone around the falling sodium drops was observed. We found that the gas temperature outside the spray cone was more uniform than expected, and the gas within the test vessel was well mixed by the natural convection due to the temperature difference between the inside and the outside of the spray cone.

(3) The sodium spray burning rate determined from the oxygen consumption rate was 160 g-Na/sec, if we assumed a 100% sodium peroxide producing

reaction in the burning. This value is equivalent to about 30% of the sodium spray flow rate of 510 g-Na/sec. We further found that the oxygen concentration did not differ significantly in the vertical direction, and the gas has been well mixed.

(4) The aerosol concentration was about 20 g-Na/m^3 at its maximum in the early stage and decreased to 1 g-Na/m^3 after 20 minute.

(5) The gas flow velocity was determined by taking the correlations of the output fluctuation between two adjacent thermocouples. Patterns during the sodium spray were found to show the complicated influence of turbulence.

Acknowledgements

We express our deep gratitudes to Mr. K. Sasaki, Mr. S. Miyahara, Mr. Y. Katogi and Mr. K. Kawata of the Plant Safety Engineering Section for their technical cooperation with us in this experiment.

References

1) S. Miyahara, et al. : "Analysis of Sodium Spray Fire (11)," (in Japanese) PNC ZN241 83-10 (July, 1983).
2) Yagi, et al. : "An Integrity Test on the Primary Containment System," (in Japanese) PNC SJ222 78(1) (July, 1977).
3) Yagi, et al. : "An Integrity Test on the Primary Containment System," (in Japanese) PNC SJ222 77-78(2) (July, 1977).

Table 1.1 Comparison of Spray Fire Tests Performed in Jaspan and Design Basis Sodium Leak Accident Posturated for MONJU

	Spray Direction	Vessel Volume (m^3)	Spray Period (sec)	Average Spray Rate (g/sec)
Hitachi	upward	1.93	8-20	20-50
Mitsubishi	downward	21	60	300
OEC/PNC (Present Test)	downward	100	1800	500
'MONJU' 1/4Dt Pipe Leak of IHTS	downward	2000	3800	3000

(PSS-SFE-313)

Table 3.1 Progression of RUN-E1 Test

Time	Test Progression
9/26	
14:33	Sodium Charge in Sodium Heater Tank
15:19	Start of Heating of Sodium in Heater Tank ..... 250 °C
9/27	
9:50	Input of Stop Conditions for CENTUN
13:22	Start of Aerosol Scrubber
:31	Completion of Heating of Sodium ..... 505 °C
:42	Stop of Cover Gas Control
:50	Start of Cover Gas Control of Sodium Heater Tank
:52	Switch off of SCR Control Heater
:54	Start of Data Recording
:57	Sodium Spray Start (Flow Rate : 36.7 ℓ/min)
14:30	Sodium Spray End (Total Supplied Sodium : 1101 ℓ)
:32	Stop of Cover Gas Control of Sodium Heater Tank
:41	Change of Temperature Level of Pre-Heating of Sodium Piping (505 °C → 250 °C)
:55	Evacuation of Sedimentation Tank
15:01	Drain Remaining Sodium in Fire Suppression Bucket
:01	Stop of Aerosol Scrubber
9/28	
0:17	Start of Cover Gas Control of Test Vessel
:01	Stop of Data Recording

(PSS-SFE-314)

Table 3.2 Test Conditions of RUN - E1

Spray Conditions	
(1) Sodium Temperature	505 °C
(2) Spray Flow Rate	36.7 ℓ/min
(3) Mass of Supplied Sodium	1101 ℓ
(4) Spray Duration	30 min
(5) Height of Falling Nozzle	4.23 m
(6) Delibery Pressure at Spray Nozzle	1.5 kg/cm^2-g
(7) Mean Droplet Diameter*	1.6 mm (Surface Mean Diameter)
	2.2 mm (Volume Mean Diameter)
* These Data are obtained by the results of water spray test	
Test Vessel Conditions	
(1) Oxygen Concentration	21 %
(2) Gas Pressure	atmospheric pressure
(3) Vessel Volume	95.5 m^3
Sodium Drainage	
After an hour from sodium spray discharge, sodium temperature decreased below 400 °C and sodium was drained to the tank.	

(PSS-SFE-315)

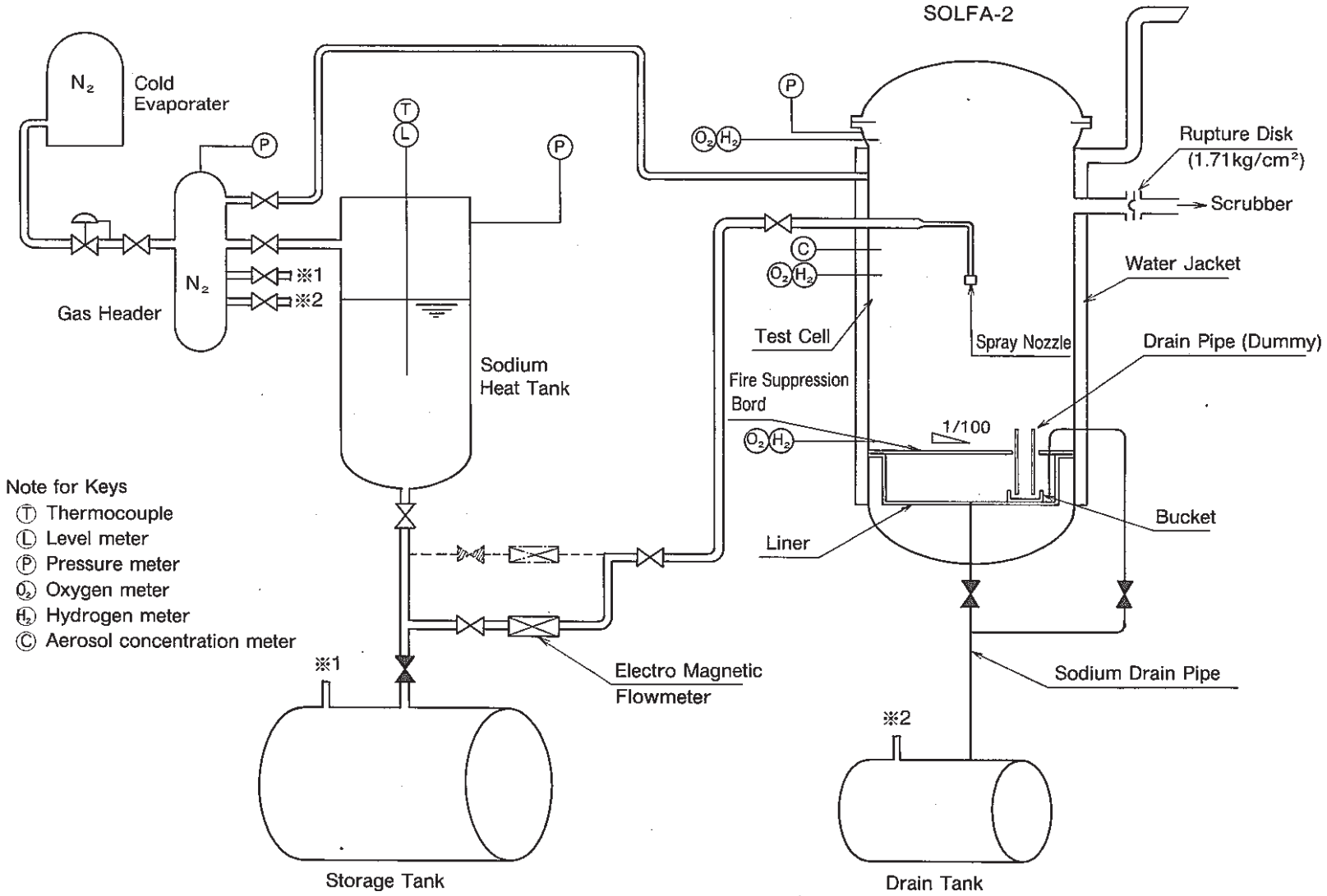

Fig.2.1 Arrangement of Test Rig for Run-E1 (PSS-SFE-316)

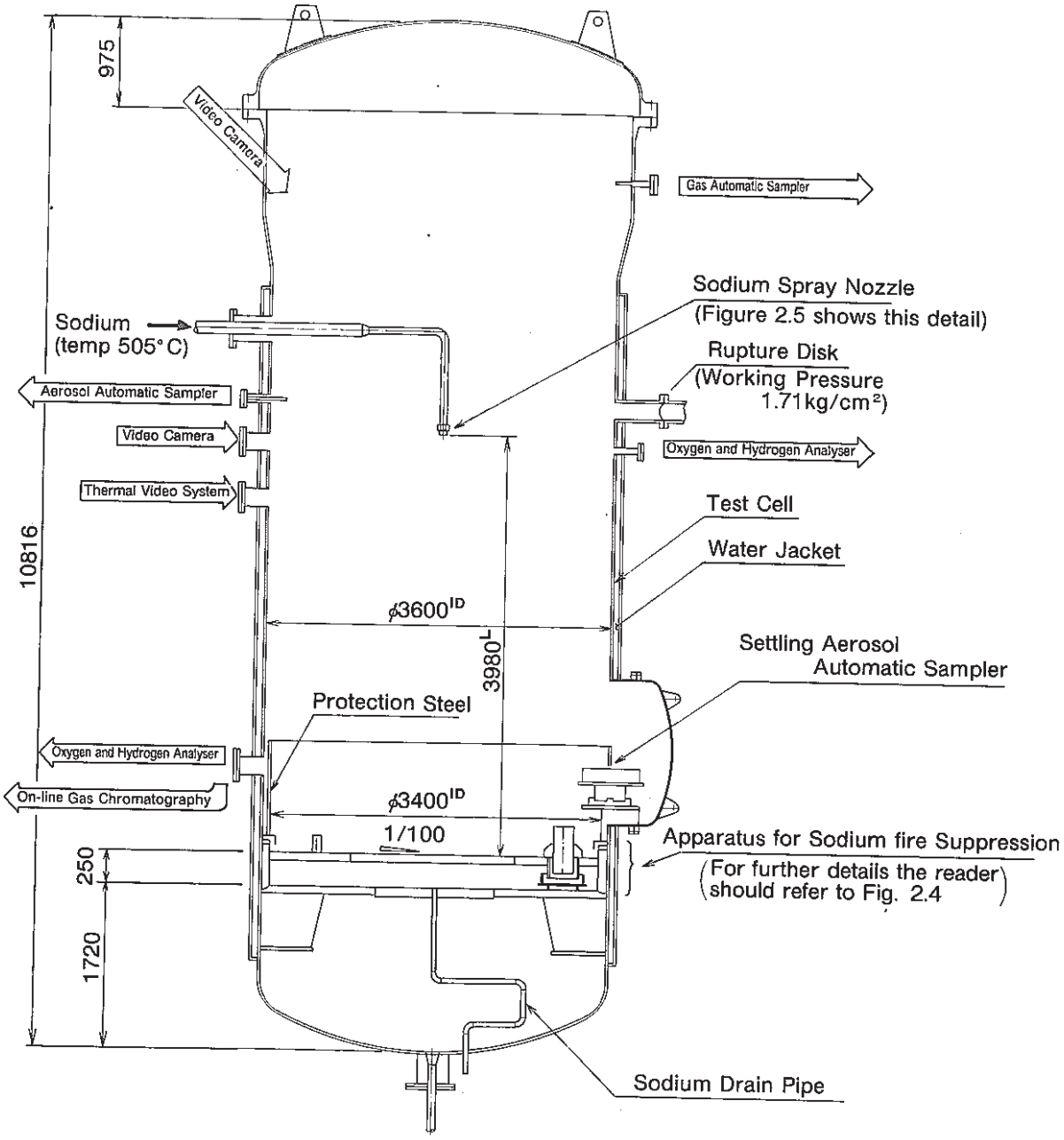

Fig.2.2 SOLFA2 Overview (PSS-SFE-317)

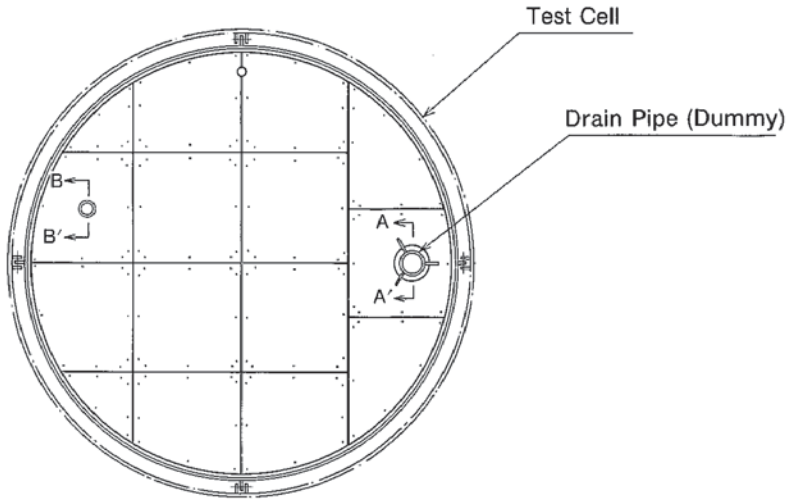

(Top View)

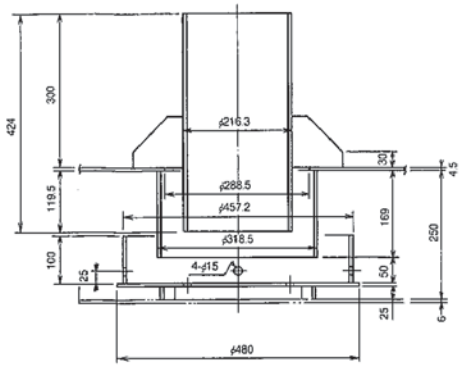

A-A description

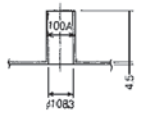

B-B description

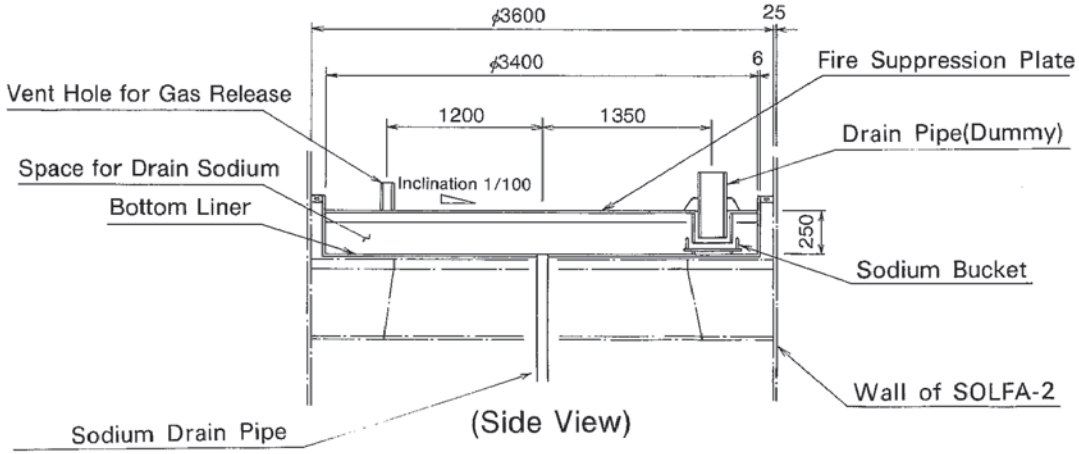

(Side View)

Fig.2.3 Apparatus for Sodium Fire Suppression (PSS-SFE-318)

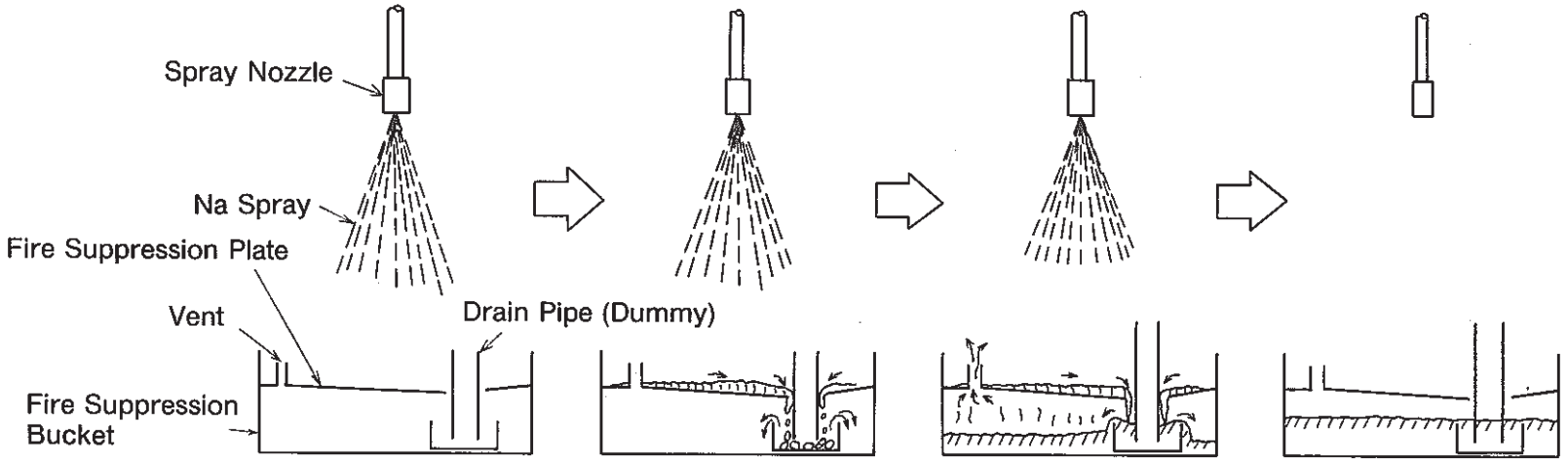

(1) Sodium has been sprayed at the flow rate of 39 ℓ/min from the nozzle.
○ Sodium Temperature 505°C
(2) Sprayed sodium has falled down on the fire suppression plate.

(1) Sodium has flowed into the drain pipe along a decline of the plate.
(2) Sodium has flowed down through a gap between the drain pipe and the fire suppression plate and gathered in the bucket.

(1) Excessive gas equivalent to a volume of sodium inflow and thermally expanding gas has been relieved through the vent.

(1) Sodium has stopped burning due to consumption of oxygen gas in the bucket.

Fig.2.4 Mechanism of Fire Suppression (PSS-SFE-319)

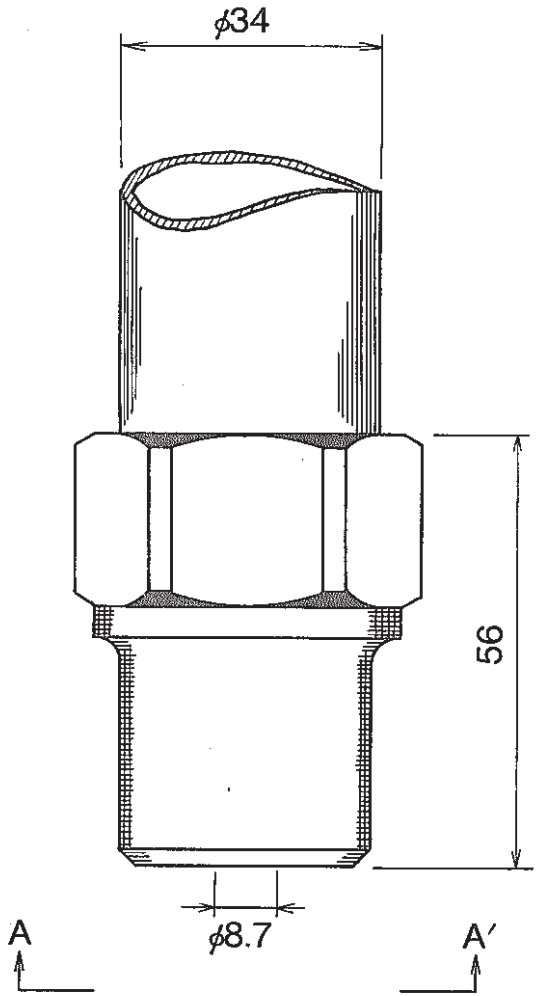

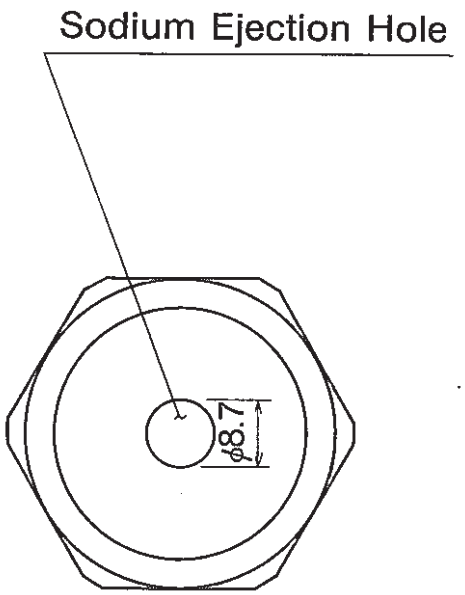

A-A′ View

Fig.2.5 Spray Nozzle (PSS-SFE-320)

Test Results (Water)

( ) : Calculated as a sodium

	Condition
Nozzle Type	1EX4400-0N
Spray Patern	Full Cone
Pressure	1.5 kg/cm²
Flow Capacity	33.5 ℓ/min (36.7 ℓ/min)
Spray Angle	35°
Mean Surface Diameter	1.6 mm
Mean Volume Diameter	2.2 mm

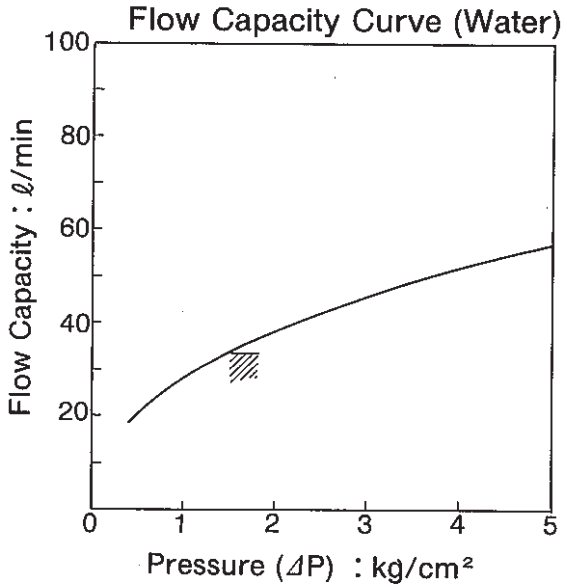

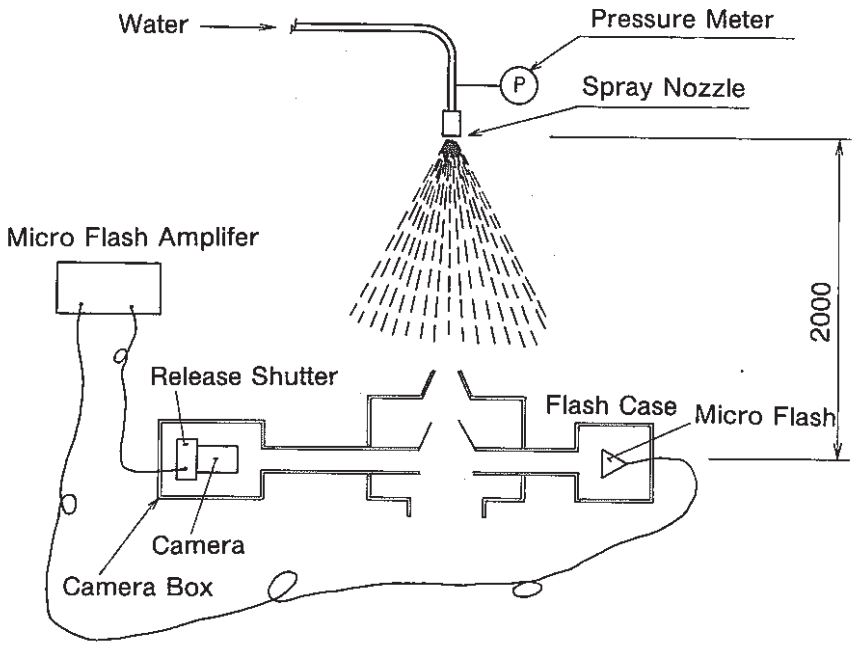

Fig.2.6 Measurement of Spray Droplets Size (Water test) (PSS-SFE-321)

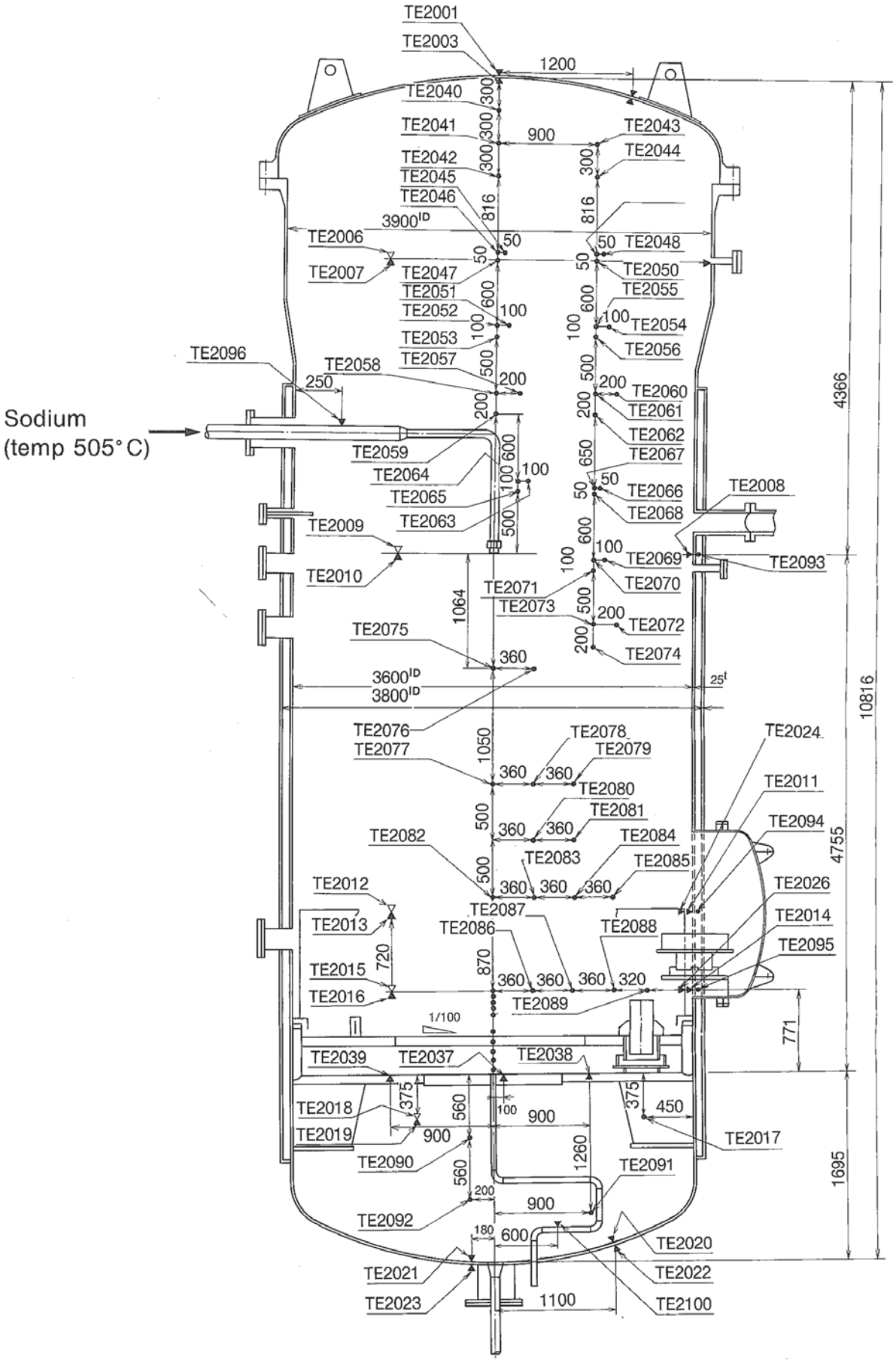

Fig.2.7 Arrangement of Thermo-couples

(PSS-SFE-322)

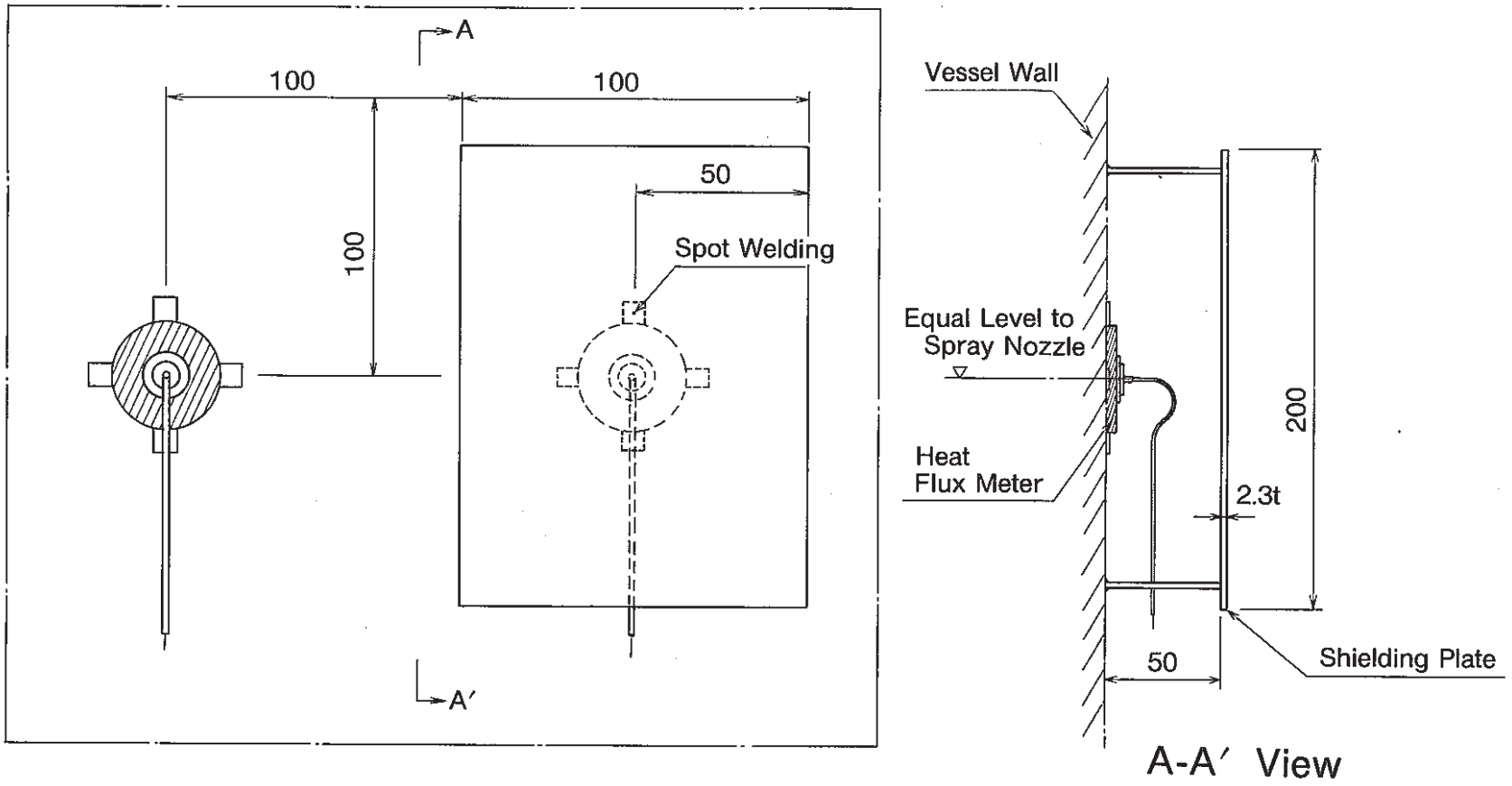

Fig.2.8 Setting of Heat Flux Meter on Vessel Wall (PSS-SFE-323)

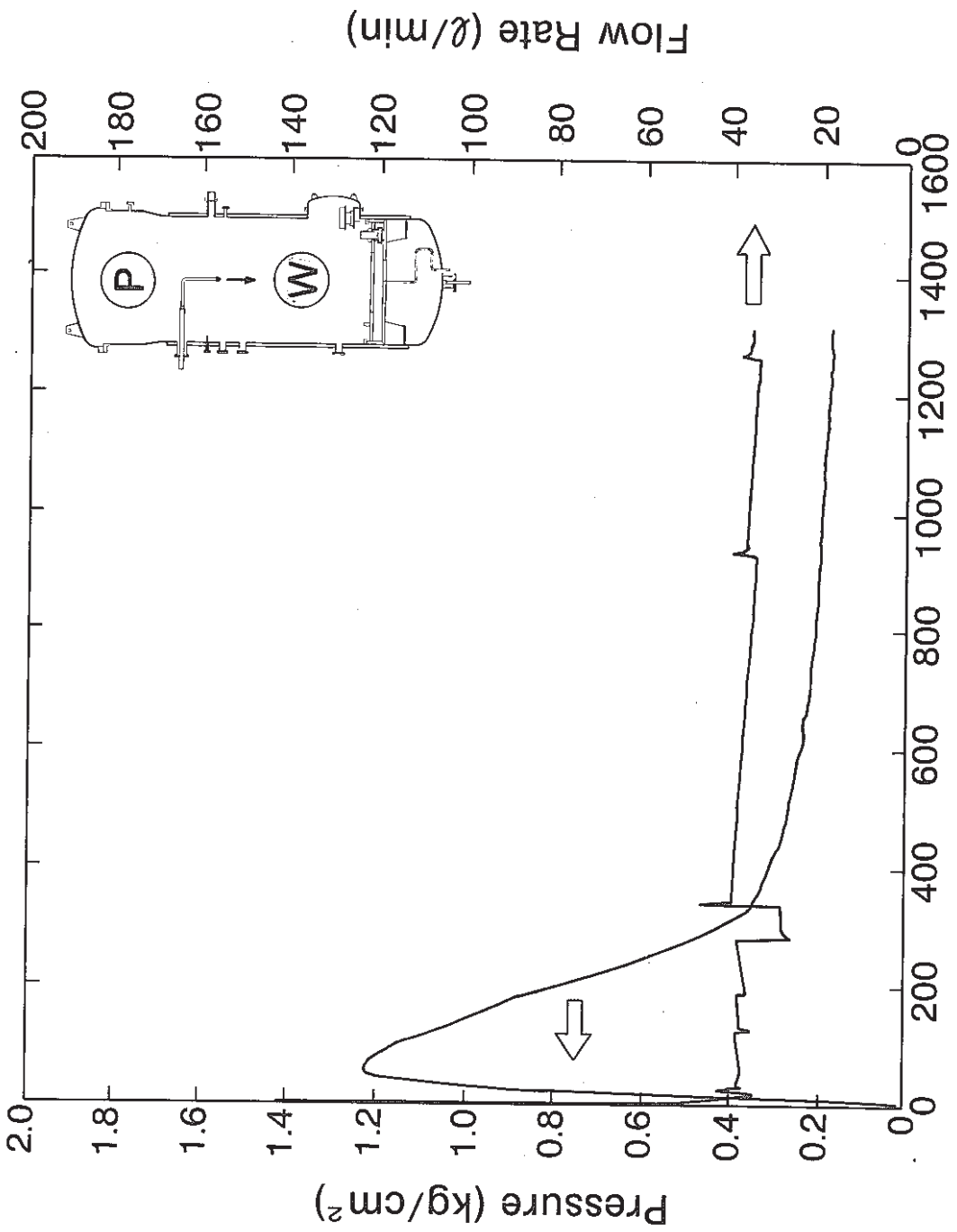

Fig.4.1 Gas Pressure and Sodium Spray Rate (PSS-SFE-324)

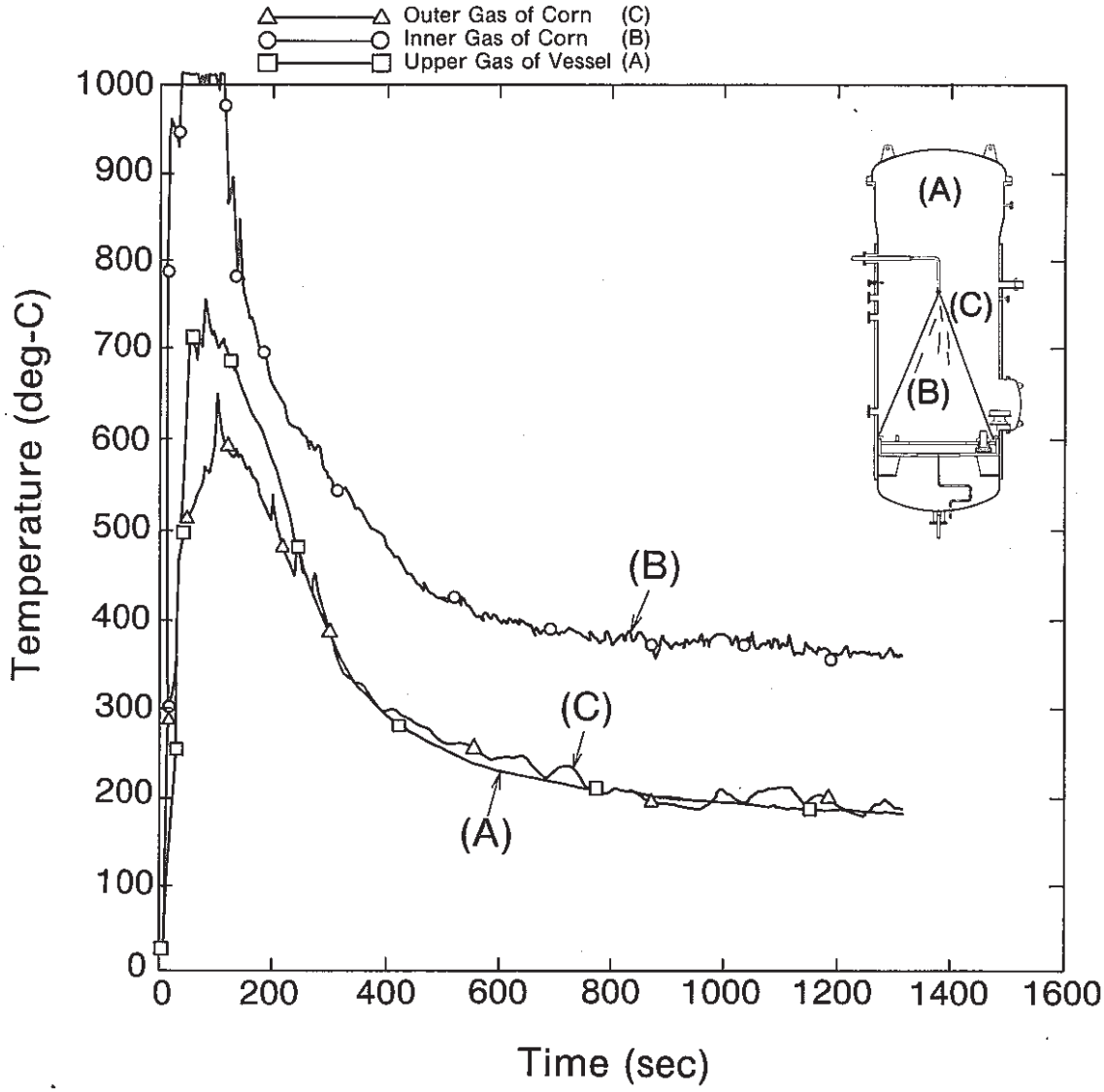

Fig.4.2 Gas Temperature (PSS-SFE-325)

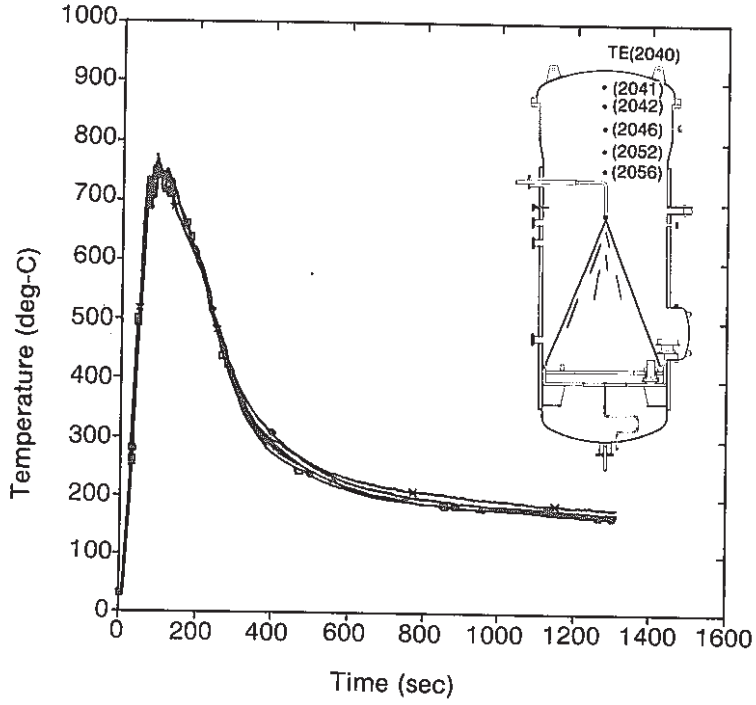

Fig.4.3 Gas Temperature above Spray Nozzle on a Center Line

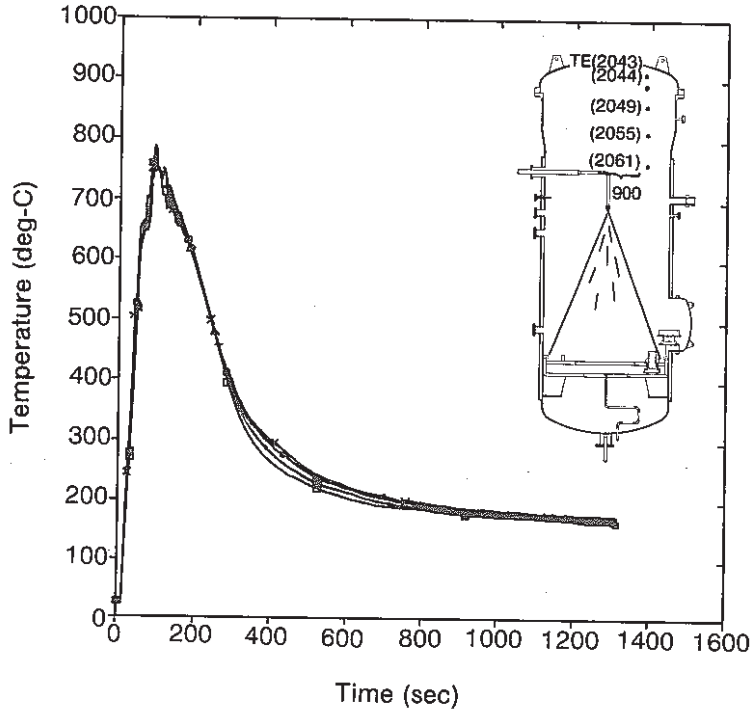

Fig.4.4 Gas Temperature above Spray Nozzle on 90 cm away from a Center Line (PSS-SFE-326)

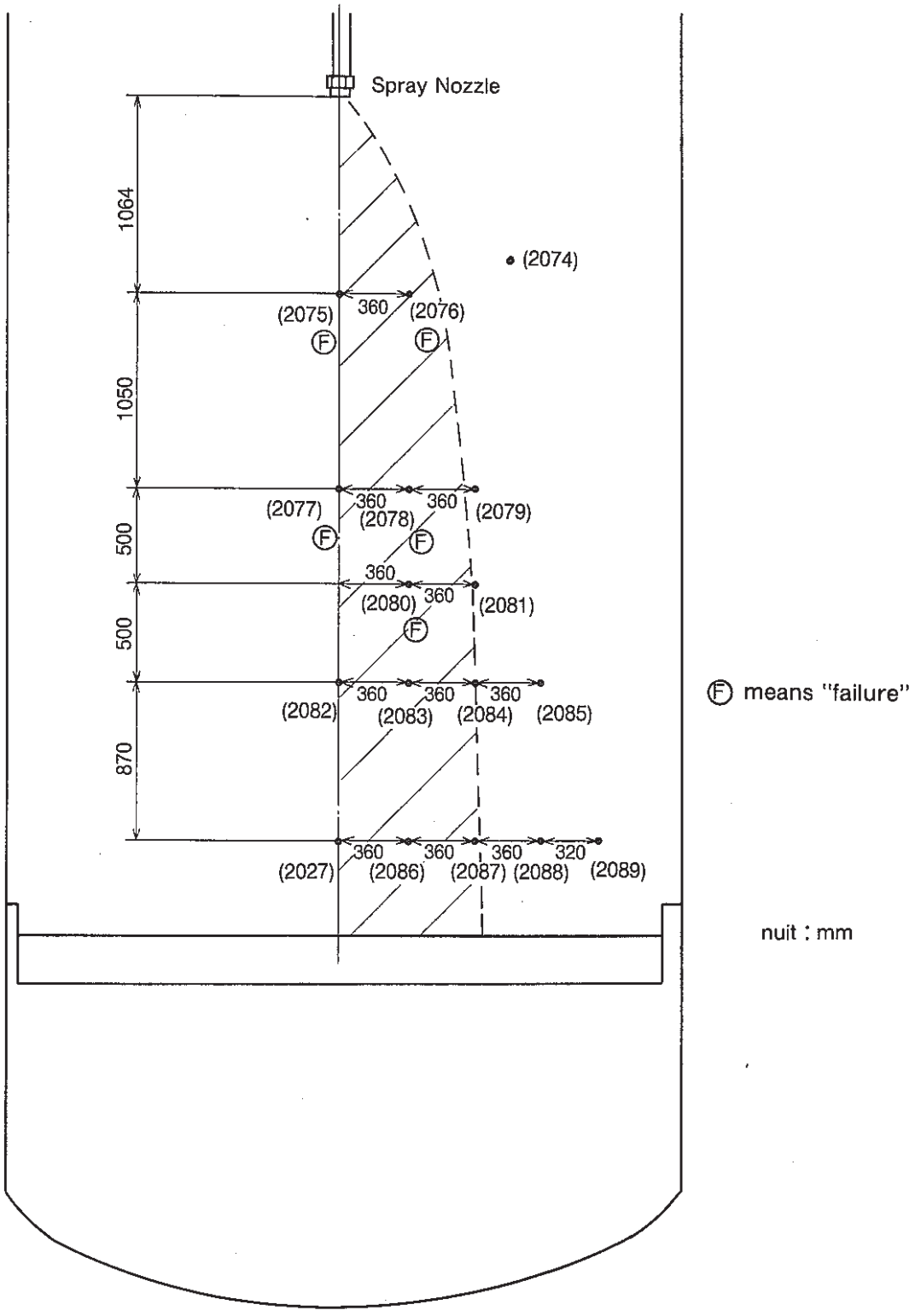

Fig.4.5 Positions of Thermo-couples below Spray Nozzle (PSS-SFE-327)

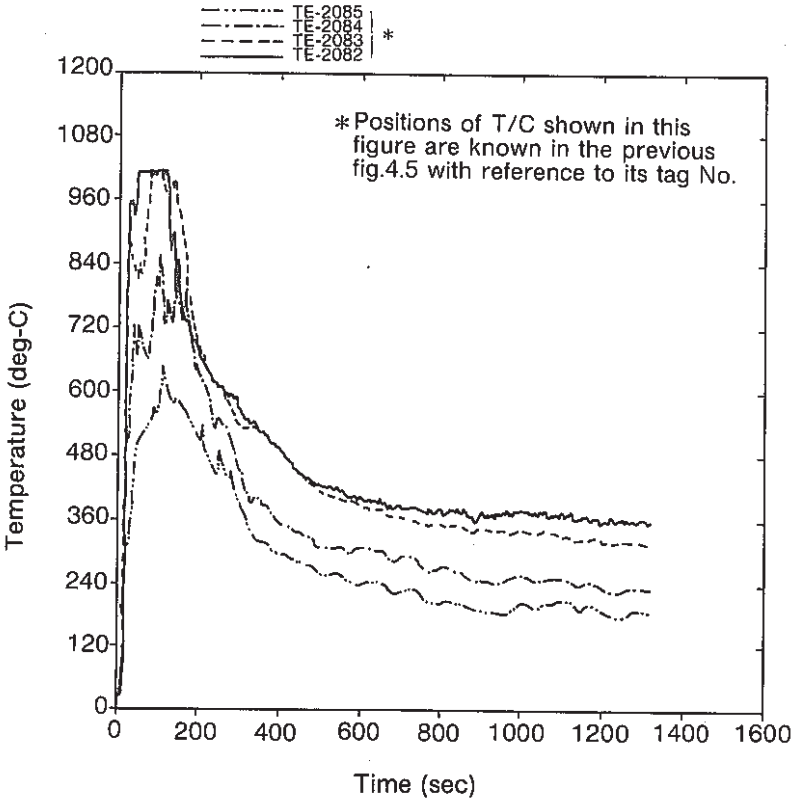

Fig.4.6 Temperature Below Spray Nozzle (3.114m down from spray nozzle)

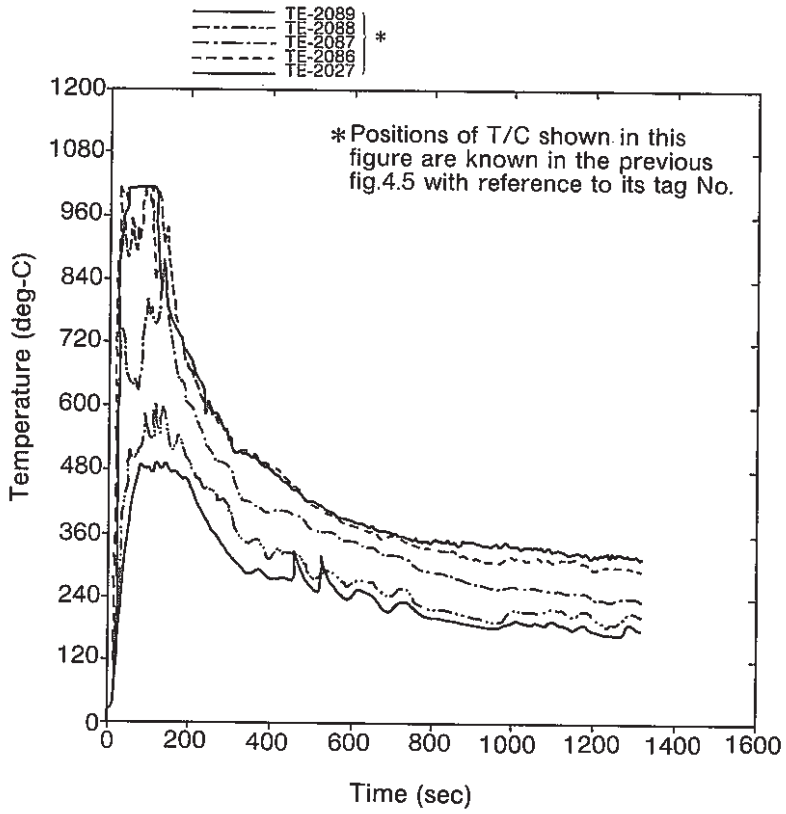

Fig.4.7 Temperature Below Spray Nozzle (3.984m down from spray nozzle) (PSS-SFE-328)

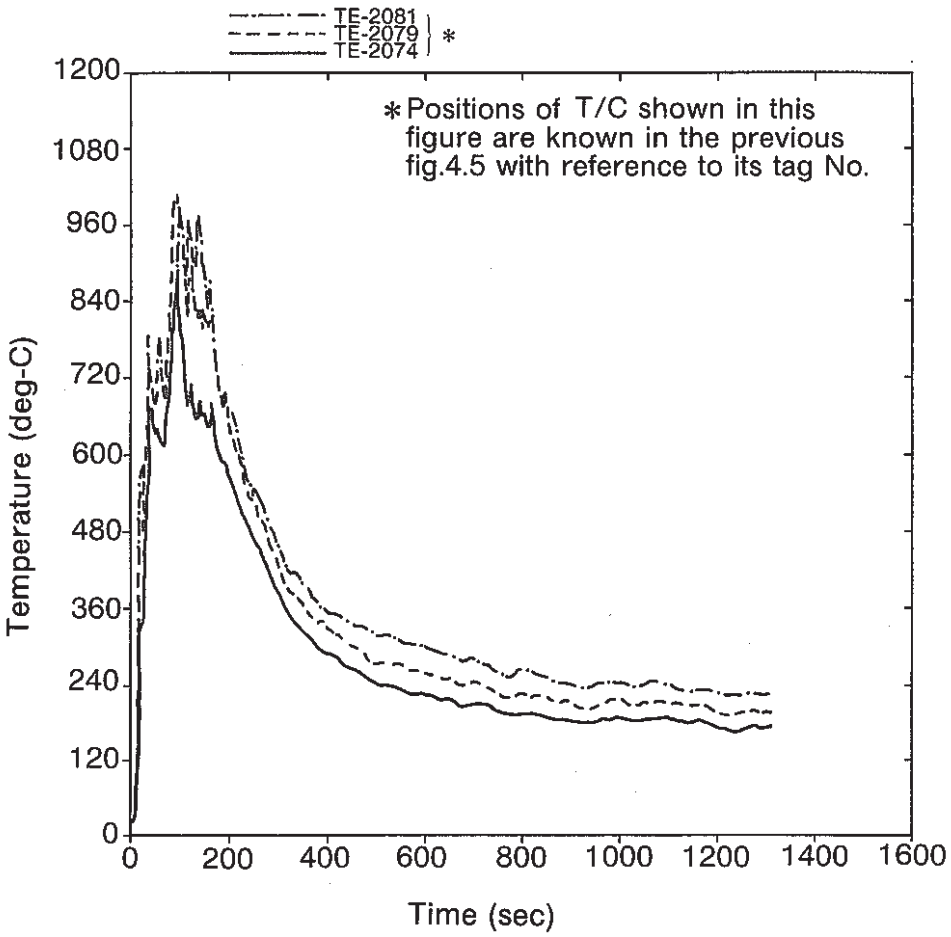

Fig.4.8 Temperature Below Spray Nozzle (the rest of thermocouples which have not been broken) (PSS-SFE-329)

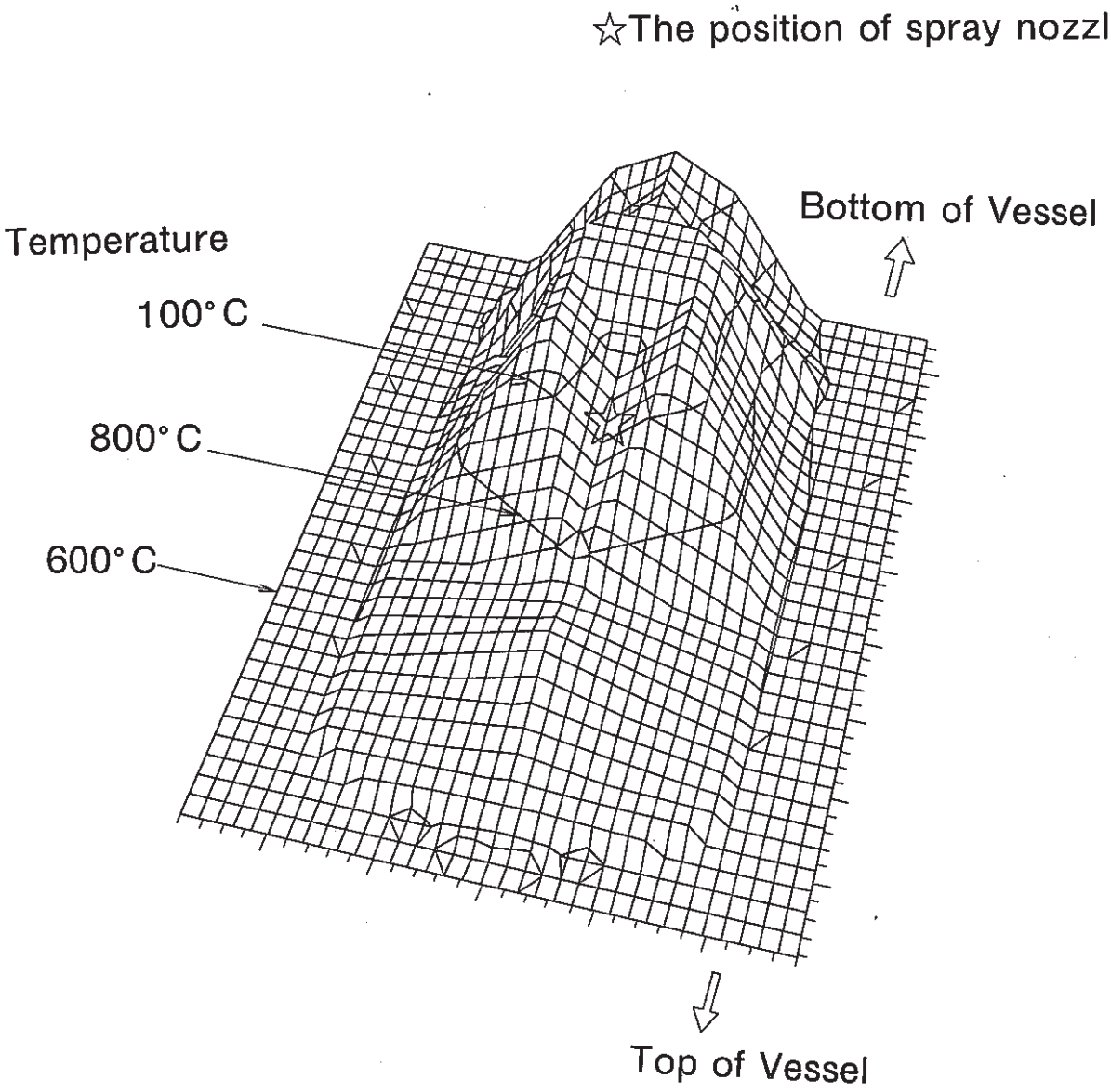

Fig.4.9 Typical Temperature Distribution of Atomosphere in Vessel (at 40 sec after spray discharge)

(PSS-SFE-330)

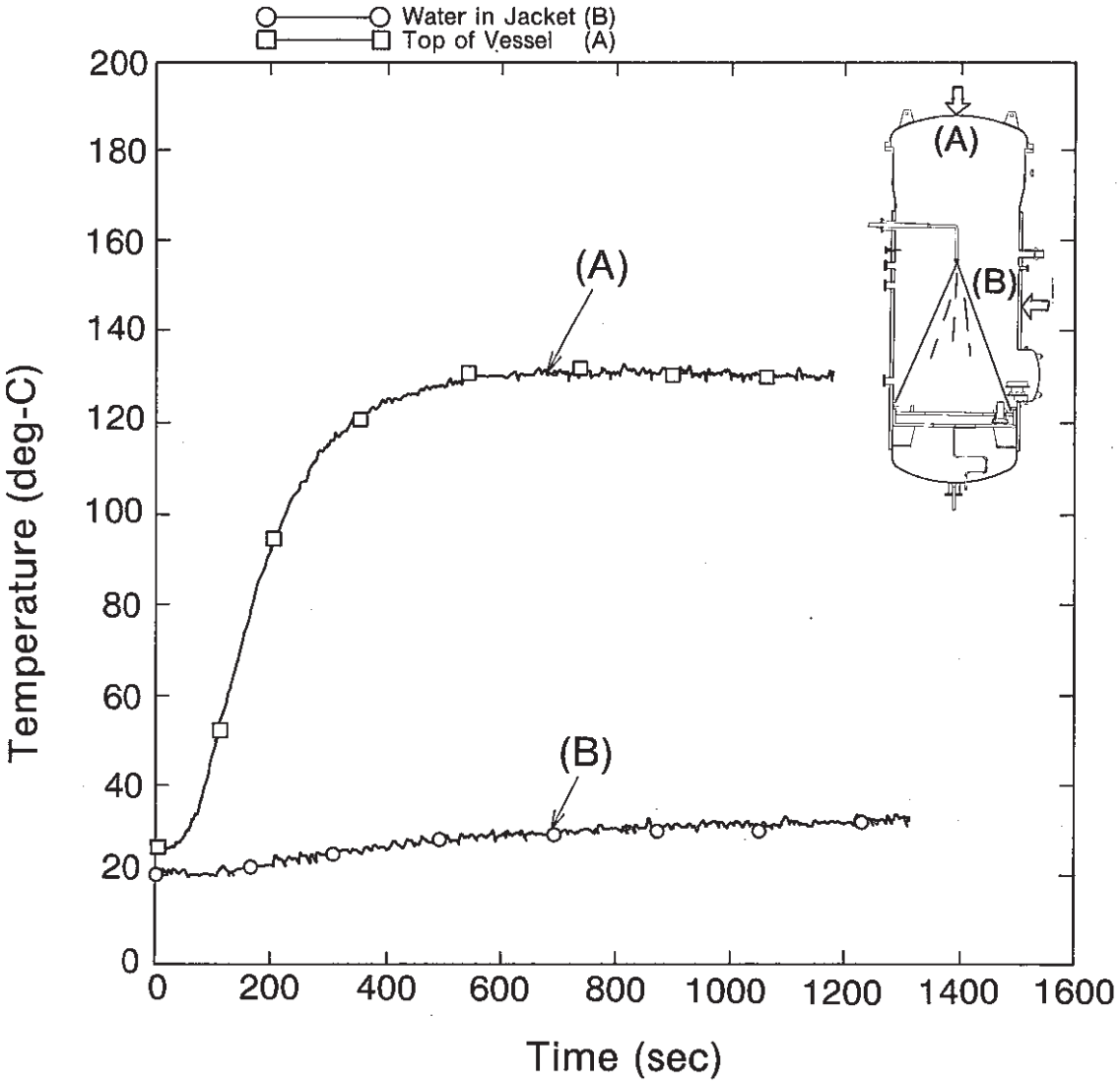

Fig.4.10 Outside Wall Temperature of Vessel

(PSS-SFE-331)

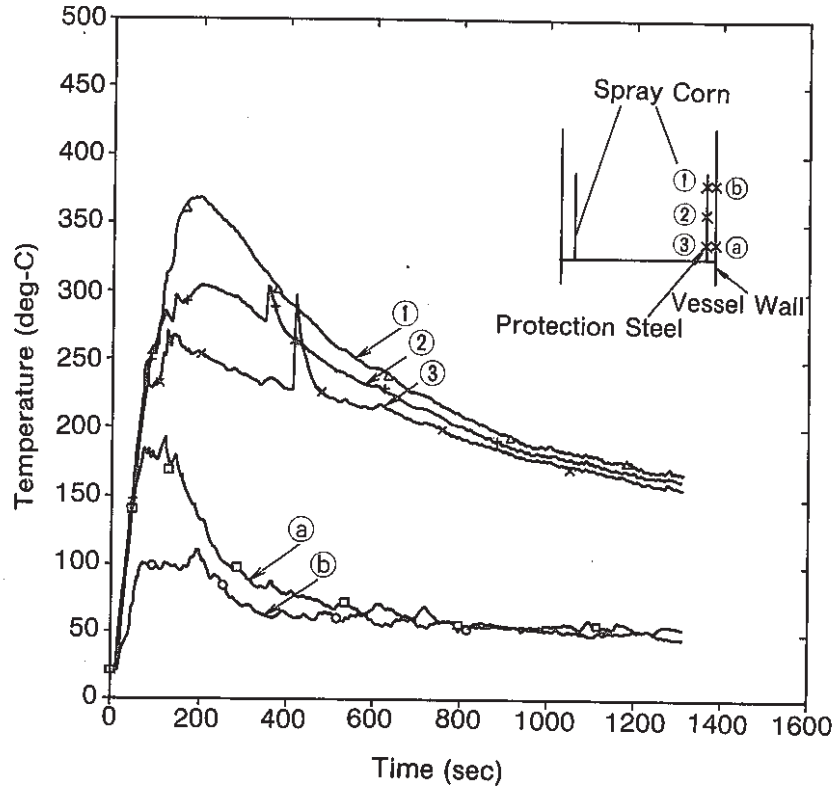

Fig.4.11 Protection Steel

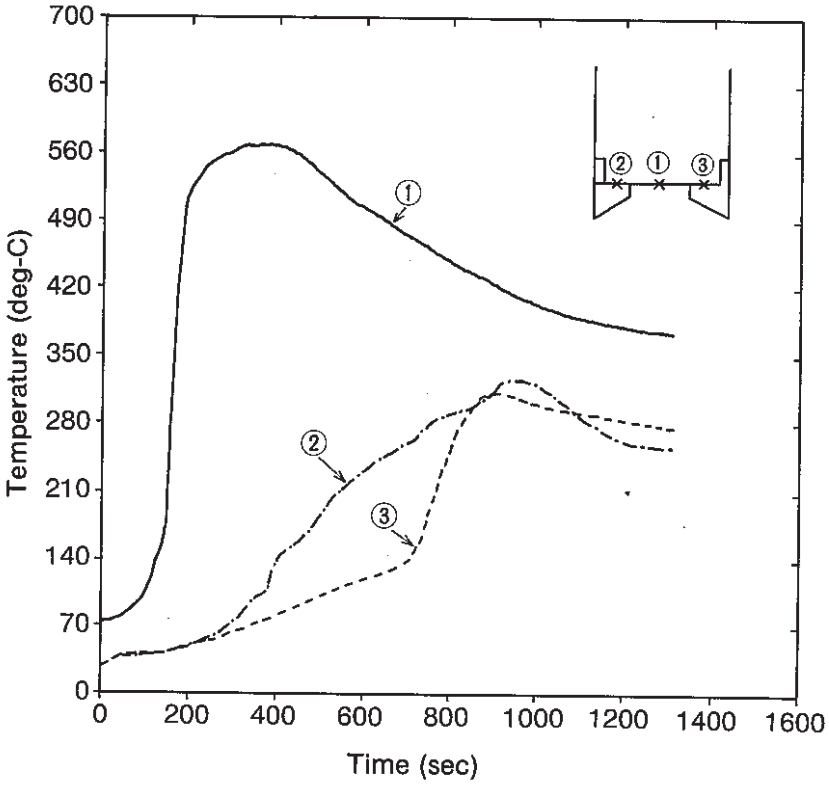

Fig.4.12 Temperature Below Catch Pan (PSS-SFE-332)

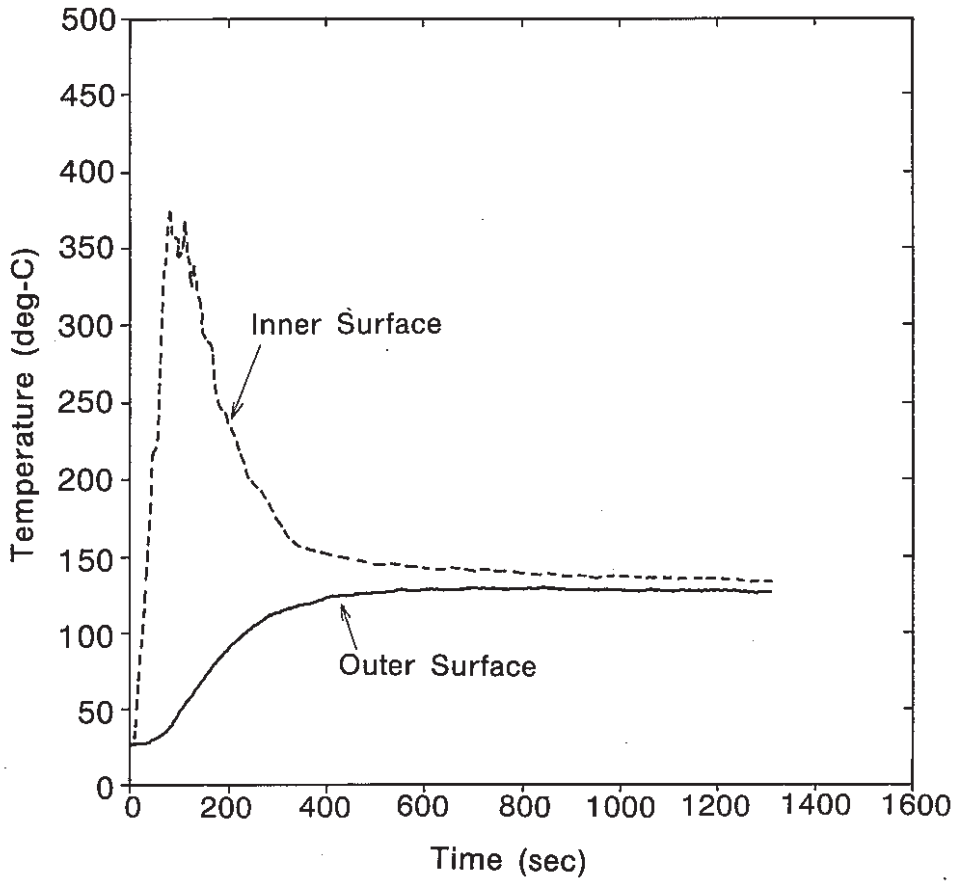

Fig.4.13 Inner and Outer Surface Temperature of Vessel Ceiling

(PSS-SFE-333)

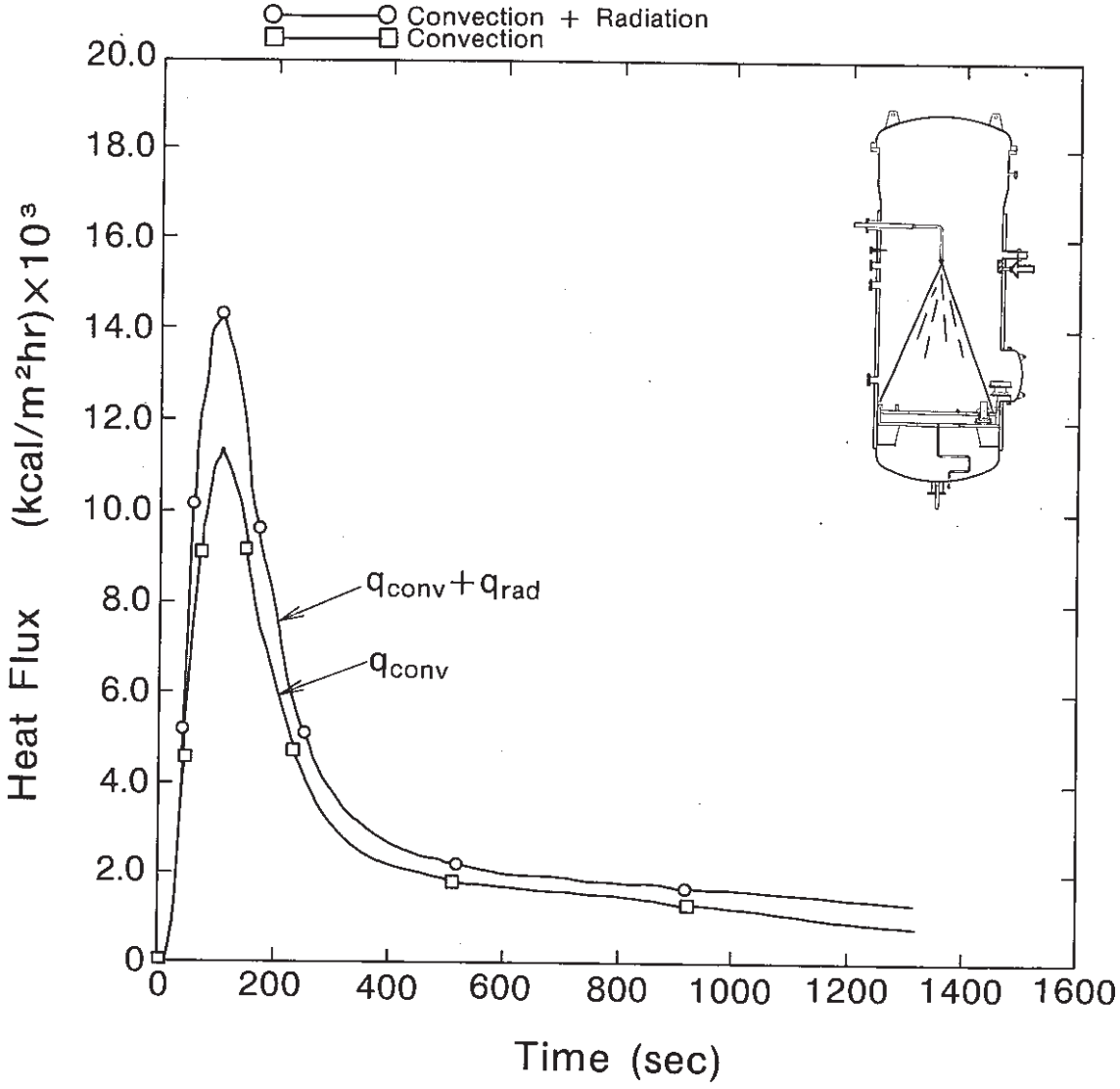

Fig.4.14 Heat Flux to Vessel Wall (PSS-SFE-334)

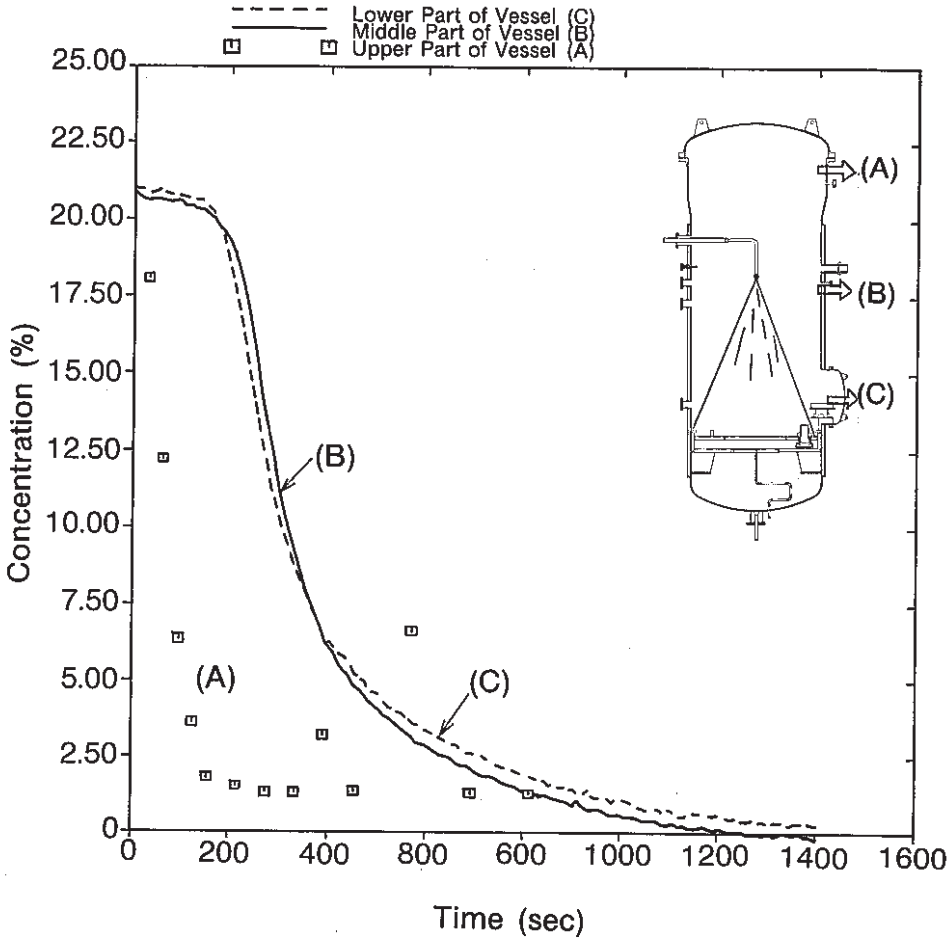

Fig.4.15 Oxygen Concentration
(Data (A) from Gas Automatic Sampler
Data (B), (C) from Oxygen Meter)

(PSS-SFE-335)

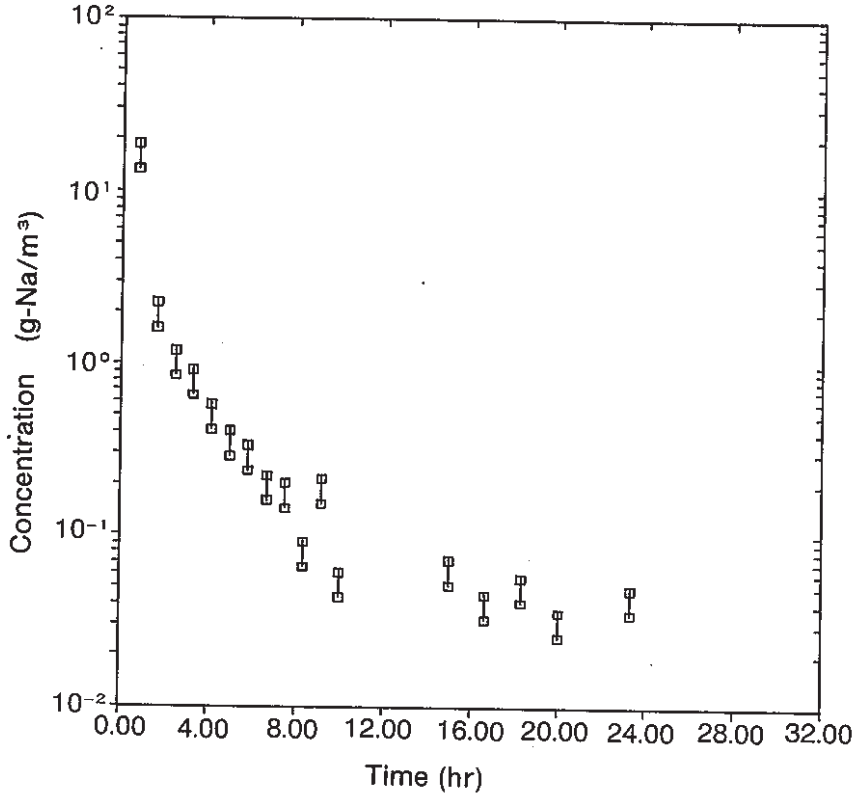

Fig.4.16 Sodium Aerosol Concentration

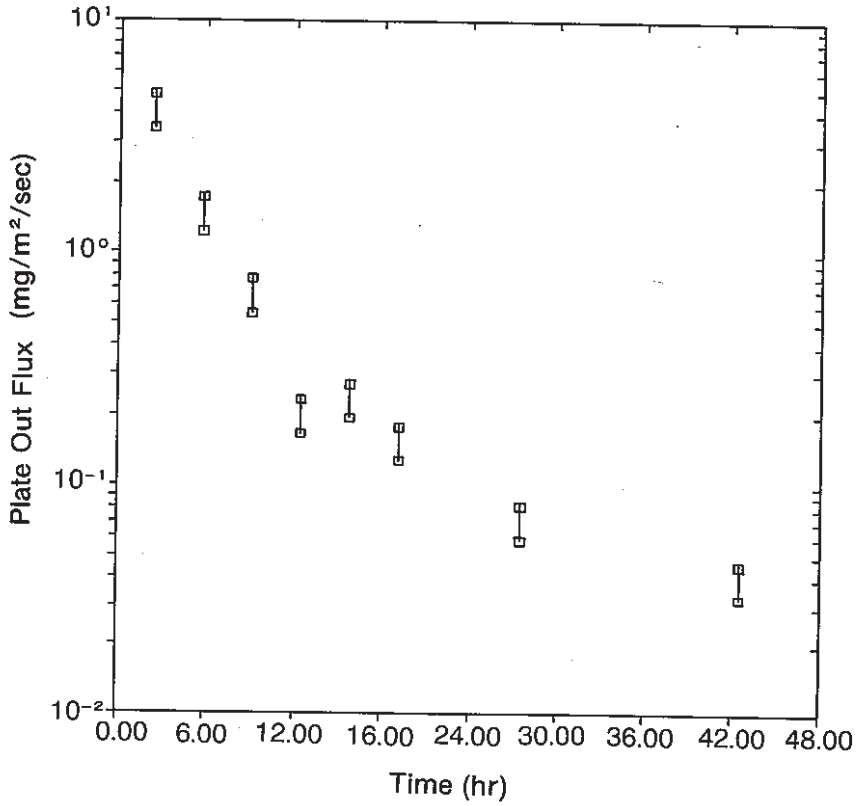

Fig.4.17 Sodium Aerosol Plate Out on Floor (PSS-SFE-336)

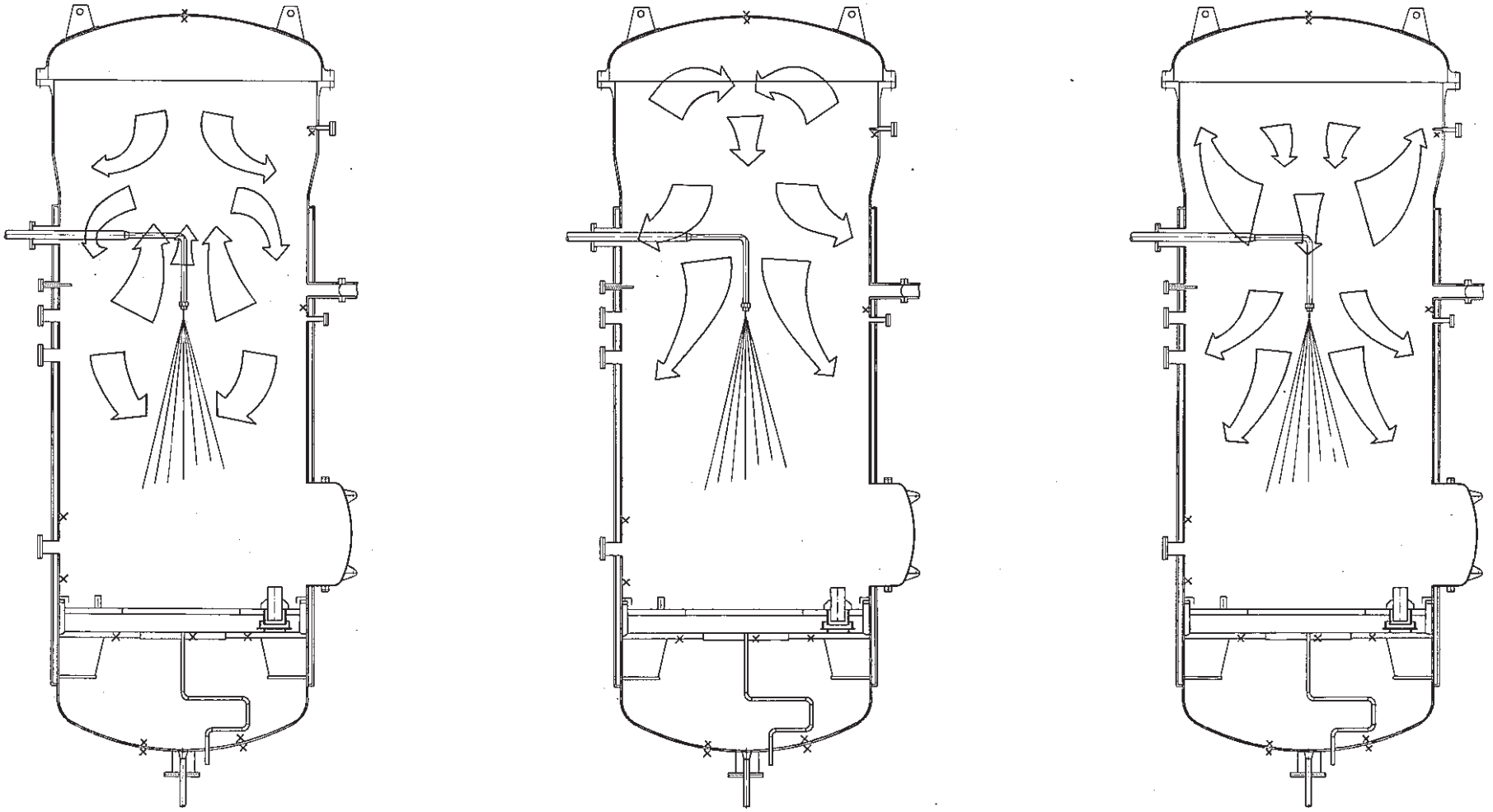

(1 min) (2.5 min) (5 min)

Fig.4.18 Gas Flow Pattern (1) (PSS-SFE-337)

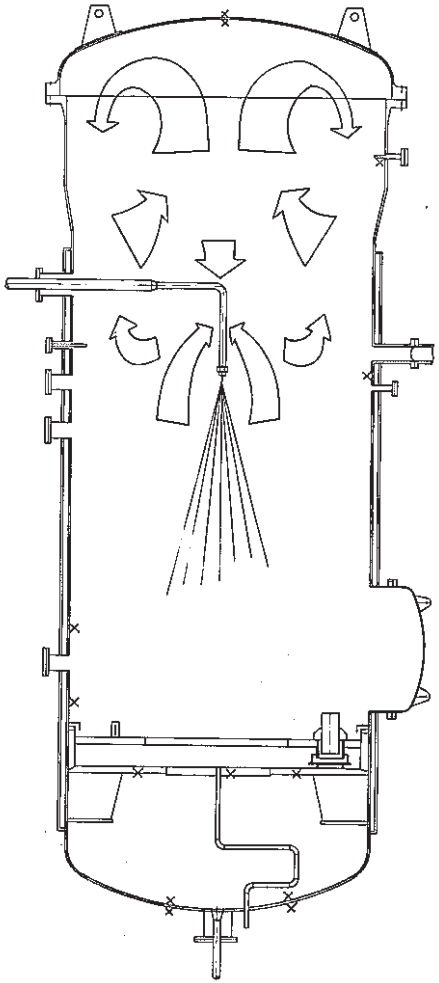

(10 min)

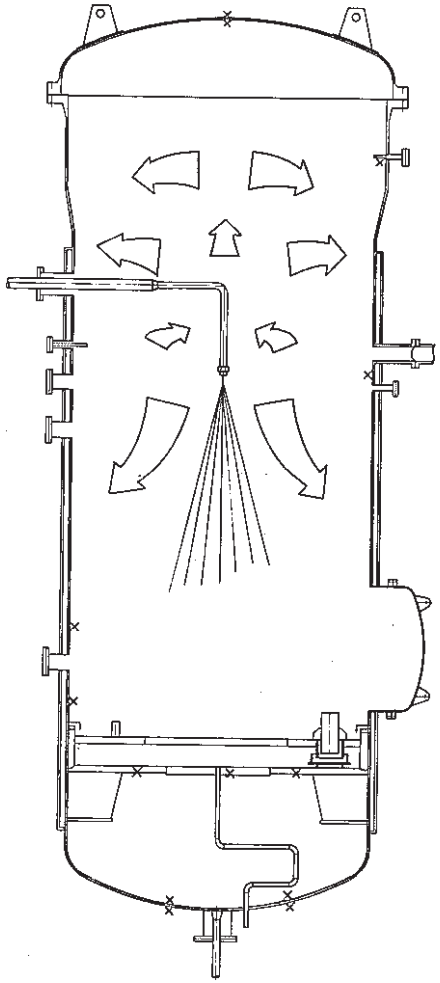

(20 min)

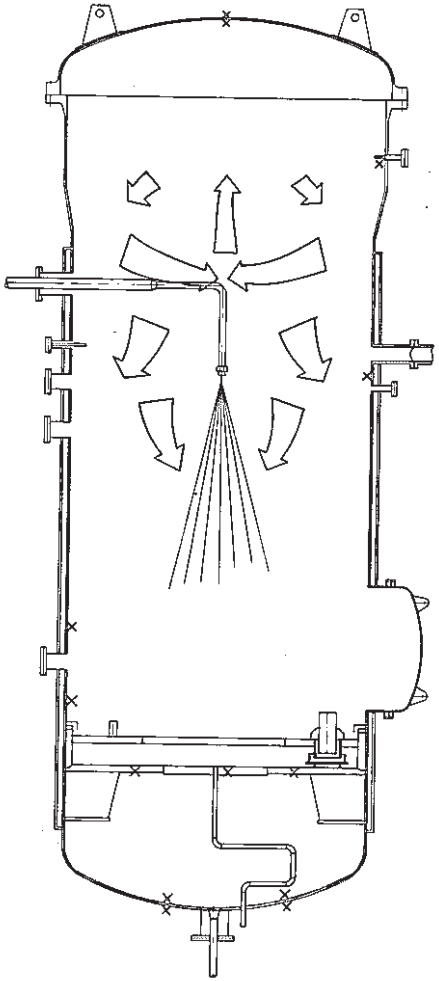

(27 min)

Fig.4.19 Gas Flow Pattern (2) (PSS-SFE-338)

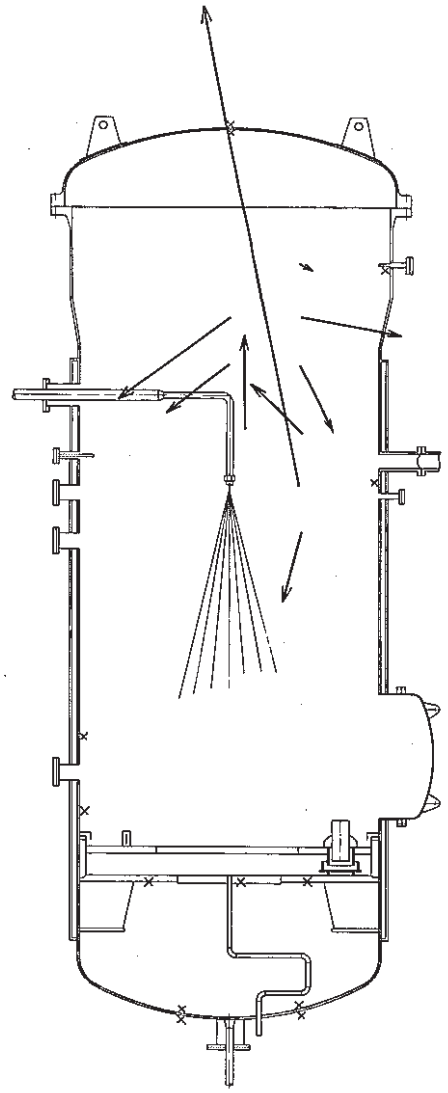

(1 min)

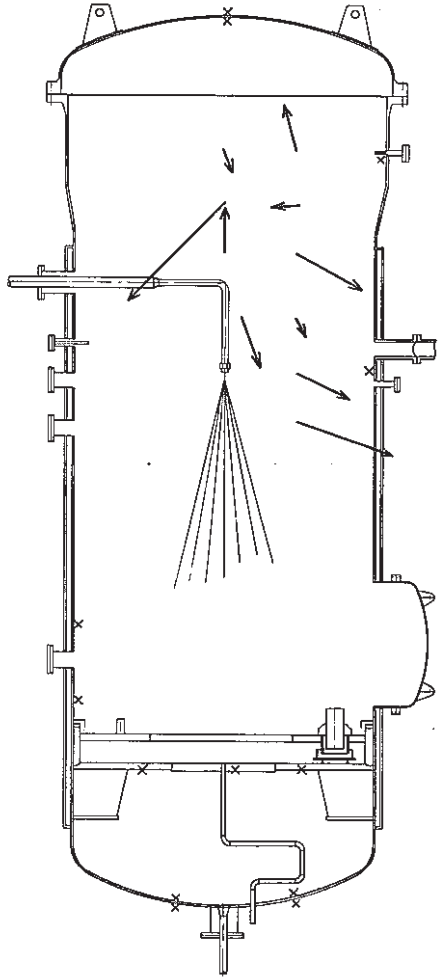

(2.5 min)

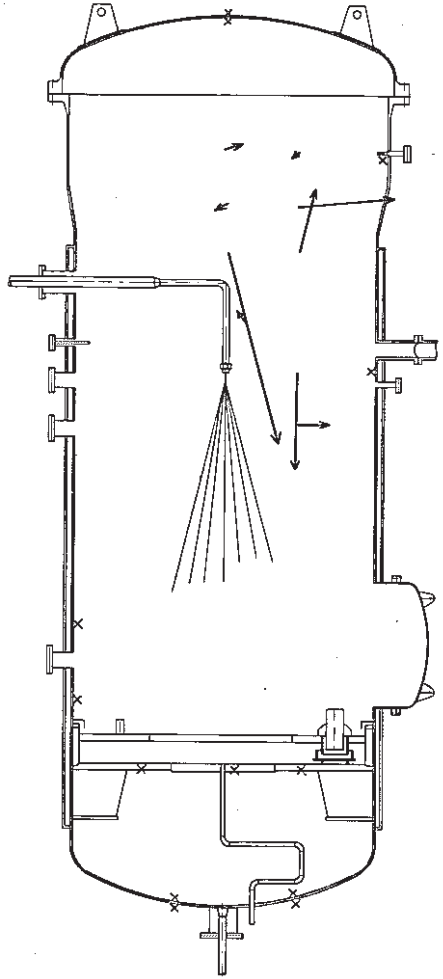

(5 min)

[➡ 1m/s]

Fig.4.20 Gas Flow Vector (1) (PSS-SFE-339)

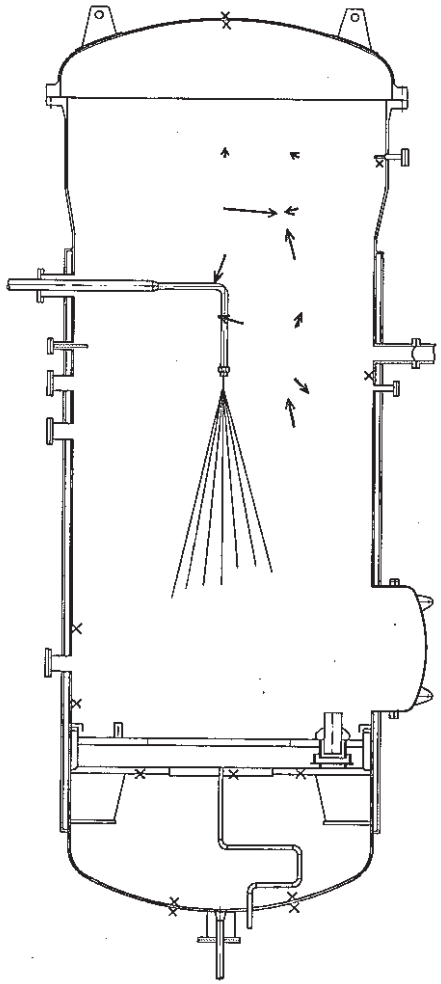

(10 min)

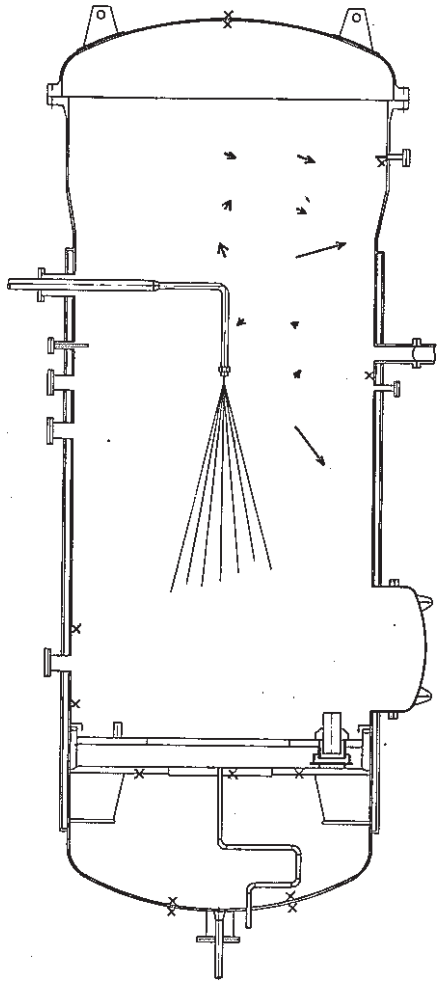

(20 min)

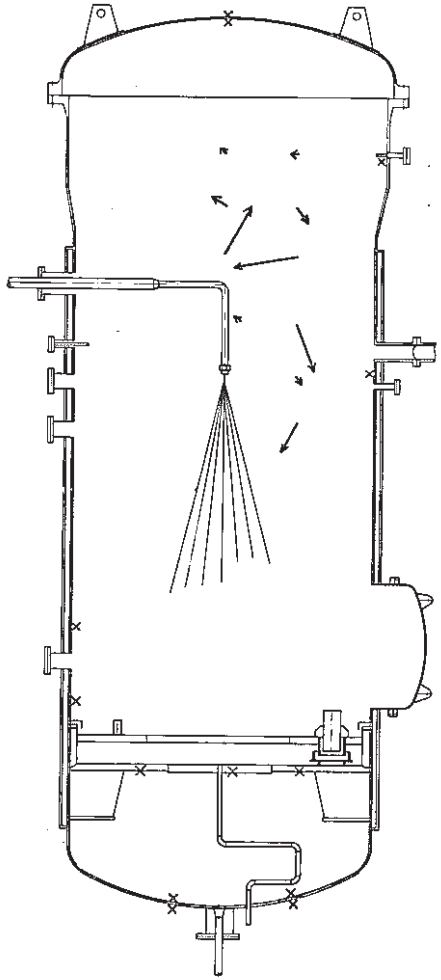

(27 min)

[➡ 1m/s]

Fig.4.21 Gas Flow Vector (2) (PSS-SFE-340)

Appendix A: Response delay of detecting oxygen concentration

Figure A-1 shows the sampling system for the magnetic type oxygen meter.

The detection delay of the oxygen meter is modeled as "Dead time" + "First-order lag," as shown below.

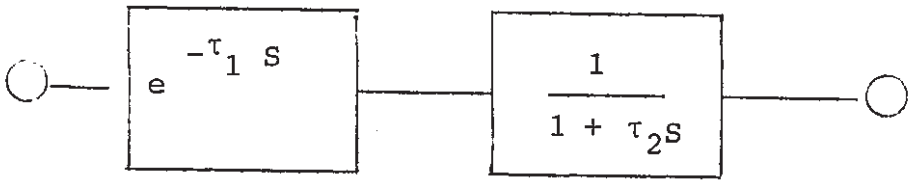

If the output is taken as y(t) and the input as x(t),

$$\tau_2 \frac{dy(t)}{dt} + Y(t) = x(t-\tau_1) \qquad \text{(A-1)}.$$

To derive the input x from the output y, one can calculate the following:

$$x(t) = \tau_2 \frac{dy(t+\tau_1)}{dt} + y(t+\tau_1) \qquad \text{(A-2)}$$

Figure A-2 shows the graph of x obtained by numerical differentiation using the test data.

The figure also shows the values of the first and second terms on the right side of the expression (A-2). The data after the complete correction is, of course, the sum of the first and second term. The figure indicates that the time

delay in the second term (i.e., the dead time in the sampling piping) is dominant.

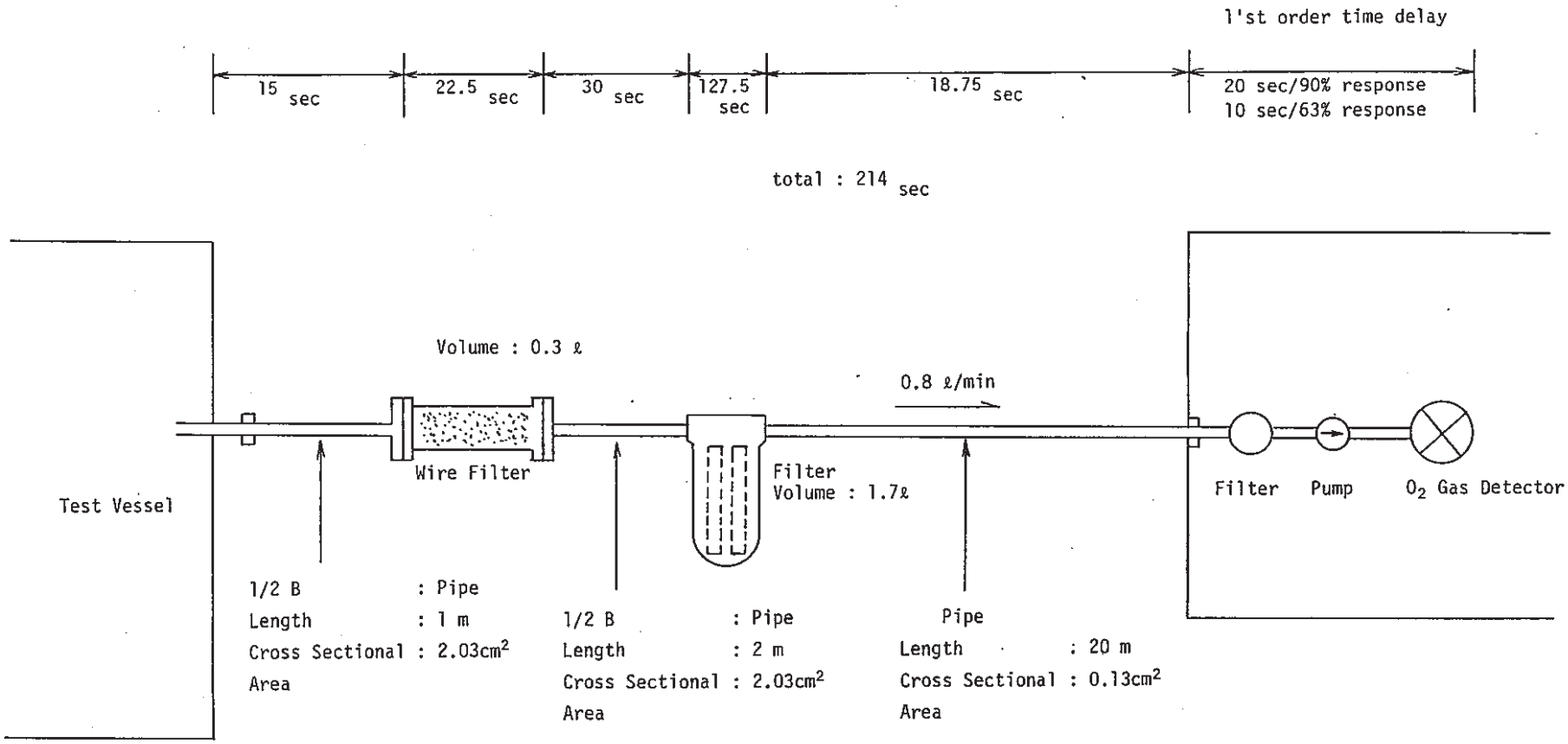

Fig.A.1 Samp 1 ing System of Oxygen Meter

(PSS-SFE-341)

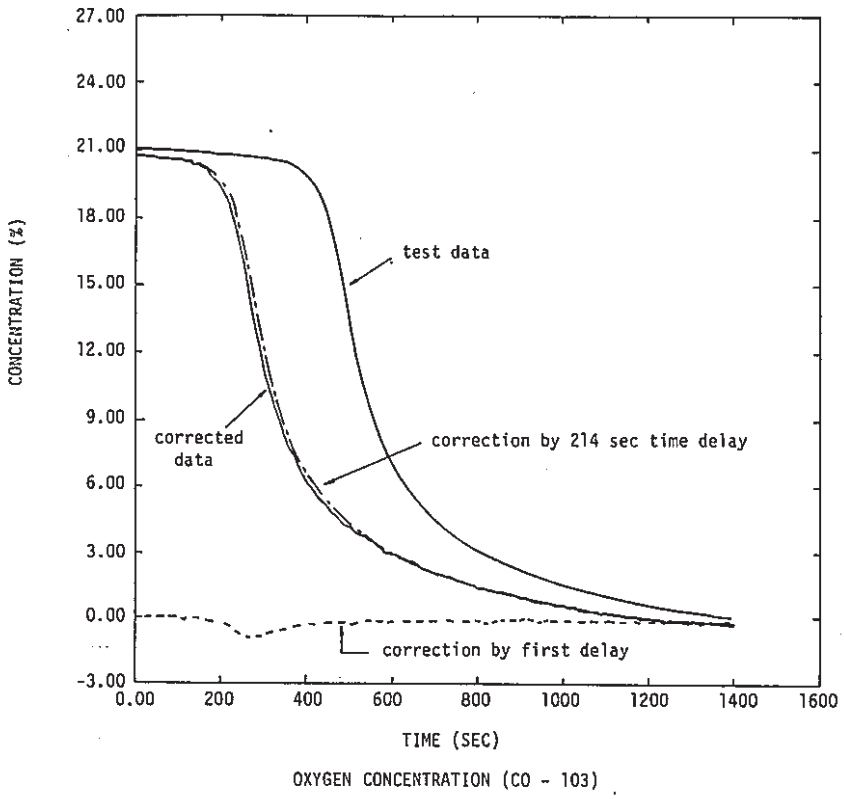

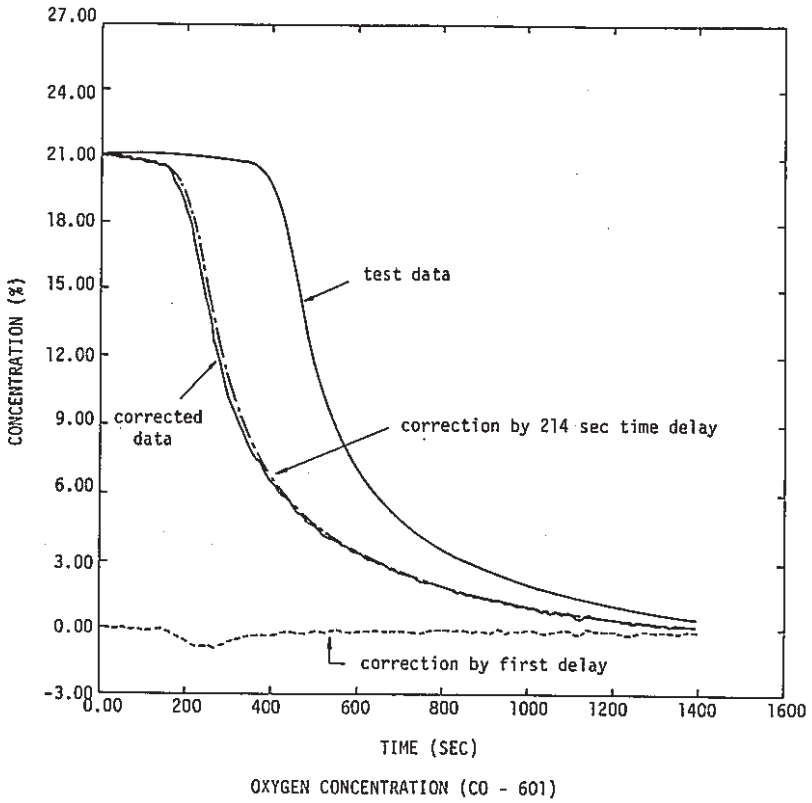

Fig.A.2 Correction of Oxygen Concentration Teat Data

(PSS-SFE-342)